UNIVERSIDADE DE LISBOA
FACULDADE DE CIÊNCIAS
DEPARTAMENTO DE FÍSICA

Texturization of ZnO:Al thin films and their application in a-Si:H thin film solar cells

Sílvia da Costa Frias de Barros

Mestrado em Engenharia Física

2009

UNIVERSIDADE DE LISBOA
FACULDADE DE CIÊNCIAS
DEPARTAMENTO DE FÍSICA

Texturization of ZnO:Al thin films and their application in a-Si:H thin film solar cells

Sílvia da Costa Frias de Barros

Mestrado em Engenharia Física

Dissertação Orientada pelos Professores Doutores:
Aldrin Antony (Universidade de Barcelona)
Maria Margarida Cruz (Universidade de Lisboa)

2009

Agradecimentos

Não estando a exagerar, muitas vezes o trabalho que tornou possível a elaboração desta tese foi duro. Por isso tenho de agradecer a uma mão cheia de pessoas que fizeram com que a aventura de a ir fazer para um país diferente se tornasse numa experiência tão positiva e enriquecedora!

Em primeiro lugar quero agradecer ao professor Aldrin Antony por tão bem ter guiado o meu trabalho e por me ter tornado uma pessoa mais confiante e sem medo. Apesar de o seu método a princípio ter sido difícil, obrigada por toda a compreensão (quando fazia asneiras), dedicação (quando mais precisei) e recompensa (quando cumpria os objectivos) demonstradas, tanto na parte experimental como na parte de escrita.

Quero agradecer à professora Margarida Cruz por toda a atenção que me deu e incansáveis sugestões para melhorar o texto da minha tese, bem como por me ter guiado pelos documentos que foram precisos até à sua entrega.

Ao professor Joan Bertomeu por me ter guiado nos primeiros dias e pela sua disponibilidade.

À Paz digo obrigada por tão bem me ter acolhido no seu gabinete e por me ter ajudado quando o meu castelhano e catalão eram tão maus que quando as pessoas falavam comigo eu respondia sim e ela respondia não (porque a resposta certa era não e eu tinha percebido uma coisa totalmente diferente!). Por me ter mostrado e explicado como tudo funcionava, inclusive como ir de encontro aos ensinamentos do professor Aldrin. Por ter sido uma amiga, me ter dado várias sugestões culturais e me ter levado a conhecer o Razz!

A todo o grupo dos almoços (Paz, Chumi, Paolo, Oriol, José Luís, ...) pelos almoços em sua companhia, pelos jantares para que me convidaram e torneios de mini ping-pong!

À Dora, Pedro e... Sukki! Sem vocês não tinha sido a mesma coisa. Obrigada pelos fabulosos fins-de-semana a conhecer a Catalunya, pelos imensos jantares à meia noite, mojitos e sessões de televisão! Por me terem dado todo o apoio das vezes que fui assaltada e por me terem dado um tecto no último mês! E obrigada ao Sukki por...me ter roubado a roupa! Ainda guardo a meia que ficou desirmanada. Ainda bem que lá estavam, adorei cada momento com vocês.

À Sonja, pelas viagens que vivemos, pelas alegrias e tristezas que partilhámos, por ser a minha companheira de ginásio e de Barcelona e me ter escutado sempre que precisava de desabafar. Por todos os sábios conselhos que me deu e planos que fizemos!

À Esther por ser uma óptima colega de casa e me ter integrado tão bem.

Quero agradecer à Catarina por me ter ido visitar e me ter dado metade da sua cama em Valência, e também à Cat por me ter dado uma cama inteira em Copenhaga!

À Marta pela hospitalidade com que me recebeu em Madrid e me ter obrigado a andar quilómetros apesar de "ser já ali! É ali já ao fundo da rua!". Da próxima vez tenho de olhar para o mapa e ver que a rua tem mais 3 quilómetros para a frente! Obrigada pela tua visita a Barcelona, passeios e aventuras que tivemos. E tenho também de agradecer seres tão boa ouvinte e uma grande amiga. Obrigada!

A todos os habitantes da residência 40 que, apesar de eu ser uma desnaturada, estão sempre ali para desanuviar a cabeça e ter conversas que me fazem sentir mais quente. Obrigada amigos.

Ao Nuno, por ter estado sempre presente quando mais precisei de apoio. Por me ter ido visitar, ter sido o meu companheiro de viagem pela Europa (sinto falta de passearmos de bicicleta e perdermo-nos e irmos parar a um sítio da cidade que não está no mapa!) e ter tantas vezes sido o meu ombro. Por ter lido várias versões da tese (apesar de não te interessar nada!) e por me ter tirado tantas dúvidas de inglês! Agradeço-te pela tua dedicação, paciência e por me fazeres sentir bem e rir. Como recompensa vou encontrar e oferecer-te um Abacate Sapo!

Por último mas com muito Amor, quero agradecer à minha família... Mãe, Pai e Inês, por me terem proporcionado esta experiência, terem sempre estado a meu lado, dado o apoio que sempre precisei de vocês e serem o meu porto seguro. E obrigada Mãe, pela comida transportável de avião!

Resumo

As necessidades energéticas da humanidade têm crescido aceleradamente, criando uma forte dependência do mundo civilizado pelas reservas de combustíveis fósseis que se sabe não serem inesgotáveis. Pelo contrário, estas são limitadas e colocam actualmente problemas ecológicos que se prendem com a produção de dióxido de carbono resultante da sua queima, que agravam e aceleram o Aquecimento Global. Este problema implica actualmente a necessidade da procura de fontes de energia alternativa, que sejam renováveis e limpas. Dentro das actualmente viáveis, a energia fotovoltaica, utilizando a radiação solar, é uma das alternativas mais limpas ainda que não suficiente para suprir de imediato as necessidades actuais. Por essa razão tem uma grande importância política, social e económica, todo o desenvolvimento que favoreça uma maior eficiência das células solares. Neste trabalho pretende-se contribuir para esse desenvolvimento, estudando a utilização de filmes texturizados de óxido de zinco dopados com alumínio para janela de entrada da luz, com o objectivo de obter uma maior eficiência de colecção da luz solar e uma melhor conversão fotoeléctrica dessa radiação.

Para esse fim, neste trabalho foram depositados por pulverização catódica assistida por magnetrão sobre substratos de vidro, filmes finos de zinco dopado com alumínio (ZnO:Al) com propriedades adequadas para serem usados como a camada de óxido condutor transparente (TCO) em células solares. O estudo da influência da texturização dos filmes finos de ZnO:Al foi realizado, recorrendo a um processo de texturização e construindo células solares do tipo p-i-n sobre esses filme finos seguindo o processo que se descreve em seguida. Todo o trabalho apresentado foi realizado na Universitade de Barcelona com o Grupo de Energia Solar.

Numa primeira fase, foi desenvolvido e optimizado um processo de limpeza dos substratos de vidro de modo a assegurar que estes se encontravam o mais limpo possível antes da deposição do TCO. Depois de se verificar que o processo de limpeza era adequado, os filmes finos de ZnO:Al foram depositados por pulverização catódica assistida por magnetrão e a texturização foi realizada através de um ataque químico com uma solução de ácido clorídrico (0,5% HCl). As diferentes texturizações obtidas foram morfológica, eléctrica e opticamente analisadas. Alguns dos filmes texturizados foram escolhidos pelas suas características e sobre eles foram fabricadas, pela técnica de deposição química de vapores catalítica por filamento aquecido (HWCVD), células

solares de filmes finos de silício amorfo hidrogenado (a-Si:H), para se estudar a influência da texturização no desempenho dos dispositivos.

Neste trabalho foi desenvolvida a montagem para a texturização e escolhidas as condições de ataque químico definindo algumas variáveis das quais a morfologia resultante depende. Os resultados para a textura são comparados entre si e o comportamento das características medidas das células de a-Si:H depositadas (curva IV, eficiência quântica, factor de preenchimento, tensão em circuito aberto e corrente de curto circuito) é relacionado com a morfologia do TCO. Apresentam-se ainda os resultados obtidos por um programa em MATLAB desenvolvido neste trabalho para se obter uma estimativa do período médio da superfície texturizada e como este valor está relacionado com os parâmetros característicos das células solares.

A estrutura do texto apresentado nesta dissertação é apresentada de seguida.

No *Prefácio* faz-se uma apresentação da importância da energia fotovoltaica e consequentemente do desenvolvimento das células solares tendo em consideração a situação energética mundial. Apresenta-se o tema do trabalho e a estrutura do texto. No *capítulo 1* faz-se uma apresentação da constituição e funcionamento das células solares bem como das suas características principais e dos parâmetros mais utilizados para classificar o seu funcionamento. Introduzem-se as diferentes gerações de células solares, as suas vantagens e desvantagens. No *capítulo 2* são explicados todos os métodos experimentais aplicados neste trabalho. Dão se os detalhes sobre o processo de limpeza do substrato, desenvolvido e optimizado no quadro desta tese, enunciando-se os protocolos definidos de forma a que o substrato de vidro esteja adequadamente limpo antes da deposição do TCO. Descreve-se o processo de pulverização catódica assistida por magnetrão utilizado para depositar os filmes de ZnO:Al e a montagem utilizada para o processo de texturização. Para estudar o efeito da texturização na qualidade das células solares, utilizou-se a técnica de HWCVD para produzir células solares sobre os diferentes TCO obtidos. Esta técnica é explicada e descrita, bem como o processo de fabrico das células solares. No *capítulo 3* são apresentados os resultados da caracterização óptica e eléctrica dos filmes atacados, bem como as suas características morfológicas. Foi ainda realizado o estudo da evolução destas propriedades em função das variáveis do ataque químico. Os resultados são comparados entre si e o comportamento das características medidas das células de a-Si:H depositadas (curva IV, eficiência quântica, factor de preenchimento, tensão em circuito aberto e corrente de

curto circuito) foi relacionado com a morfologia do TCO. Apresentam-se ainda os resultados obtidos por um programa em MATLAB desenvolvido para se obter uma estimativa do período médio da superfície texturizada e a análise de como estes valores estão relacionados com os parâmetros das células solares. No *capítulo 4* são apresentadas as conclusões a tirar dos resultados obtidos e sugeridas propostas para um estudo mais profundo e completo nesta área.

Os resultados principais deste trabalho relacionados com o papel da texturização da camada TCO são os que se descrevem em seguida:

- Com o tratamento químico, a resistência superficial (sheet resistance) de todos os filmes finos de ZnO:Al aumentou, sendo este resultado atribuído à diminuição da sua espessura. Este tratamento químico deve ser realizado numa geometria horizontal para assegurar a homogeneidade da espessura final;
- As condições de pulverização para o crescimento do filme são determinantes no processo de texturização;
- A caracterização óptica dos filmes, medindo a transmissão total e a transmissão difusa e calculando-se a fracção de luz dispersa (*"haze"*) permitiram concluir que: todos os filmes apresentavam transmitâncias superiores a 83% na banda da luz visível; a transmissão total no infra-vermelho próximo aumenta com o tempo de ataque químico; a transmissão difusa na banda de luz visível aumenta com o ataque químico, atribuído a um aumento da rugosidade da superfície;
- Para as células construídas sobre os filmes de ZnO:Al texturizados, foram analisados os parâmetros seguintes: eficiência quântica externa (EQE), densidade de corrente de curto circuito (J_{sc}) e a curva característica (IV), tendo-se concluído que:
    - A texturização realizada nos filmes ZnO:Al foi transmitida a todas as camadas da célula;
    - As células depositadas sobre filmes texturizados têm densidades de corrente de curto-circuito mais elevadas que os filmes não texturizados;
    - A melhor eficiência obtida, melhor do que as células construídas sobre substratos comercialmente disponíveis Asahi-U, foi conseguida numa célula texturizada por ataque químico durante 20s com orientação horizontal;

- Com os filmes ZnO:Al texturizados, obtiveram-se células solares com eficiências de 3,31% que devem ser comparados com o valor 3,25% obtido nas células depositadas sobre substratos Asahi-U.

Das conclusões retiradas através dos resultados obtidos, são sugeridas algumas propostas para um estudo mais profundo e completo nesta área. As condições de deposição dos filmes finos de ZnO:Al são um parâmetro crítico que determina o resultado da texturização por ataque químico. Neste estudo a melhor escolha de parâmetros incidiu em filmes depositados com uma potência r.f. de 200 W e uma temperatura de 350 ºC para o substrato. Um tratamento mais exaustivo em que sistematicamente se variem estes parâmetros poderá conduzir a filmes cuja texturização resultante seja de melhor qualidade. O tipo e uniformidade da texturização podem também ser melhor caracterizados recorrendo a estudos da distribuição angular da luz dispersa e a imagens de microscopia electrónica de varrimento em secções rectas da superfície.

Palavras-chave: Texturização de filmes finos de ZnO:Al, Texturização TCO, Confinamento Óptico, Células solares de filmes finos de a-Si:H, Deposição química de vapores catalítica por filamento aquecido (HWCVD)

Abstract

The present work was developed in Barcelona University, with the Solar Energy Group. In this work, ZnO:Al thin films with optimum properties to be used as transparent conductive oxide (TCO) contact layers in solar cells, were deposited by radio-frequency magnetron sputtering onto glass substrates. The main goal of this work was to texturize the as-deposited ZnO:Al thin films for light confinement purposes to achieve an improvement in efficiency of thin film silicon solar cells. The texturization was carried out by wet chemical etching with diluted hydrochloric acid (0,5%HCl), a simple and economic method, with which is possible to improve the light trapping in thin film silicon solar cells. Additionally, amorphous silicon (a-Si:H) thin film solar cells were deposited by HWCVD over the different achieved TCOs, to study the influence of the texturization in the devices performance.

First, a cleaning process was developed and optimized to ensure the glass substrates were very clean prior to deposition of TCO. After checking the cleaning process fulfilled the requisites, the ZnO:Al films were deposited by r.f. magnetron sputtering with optimized process conditions. The texturization set-up was developed, the etching conditions were chosen and the films were etched changing some variables on which the resulting surface morphology depends. The properties of the different resulting textures were morphologically, electrically and optically analyzed. Using the experimental results, some textured films were selected to built a-Si:H solar cells over them. The performance of such solar cells was related with the morphology of the TCO layer. A MATLAB program was developed within the project to find out the average period of the textured surface and how these values are related with the parameters of the solar cells.

The effect of the different textured TCOs in the performance of the deposited a-Si:H solar cells were analyzed and compared. From the conclusions taken are suggested proposals to do a more deep and complete study on this area.

Keywords: ZnO:Al thin films texturization, TCO texturization, Light trapping, a-Si:H thin film solar cells, hot wire CVD

Table of Contents

List of figures

List of tables

Preface

The huge dependence of humanity on fossil fuels and its fast depletion, demand the world to search for alternative and renewable energy sources. The economic, social and political instabilities, limited resources, and war conflicts with countries which have greater fuel reserves lead to the rise of fossil fuel prices. Figure 1 shows the share of total primary energy supply in 2006. Besides the politic and economical problems associated with the use of fossil fuels, they also produce gases that worsen the greenhouse effect leading to Global warming. Because of this, it is crucial to use renewable energy sources like wind, water, geothermal and solar energy, which also have the advantages of being environmental-friendly, virtually unlimited and spread over the entire planet.

Because the global warming's alarming impacts, the European Union has committed itself to accelerate the reduction of the greenhouse gases (GHG) through the *20- 20-20 programme by 2020* package. The programme aims to reduce carbon dioxide emissions by 20% below 1990 levels, increase to 20% by 2020 the renewable energy share of the total energy mix and improve energy efficiency by 20 percent by 2020.

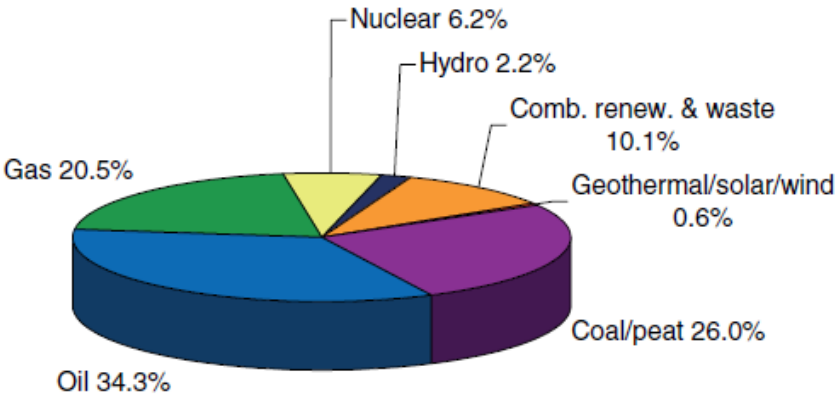

Figure 1 Share of total primary energy supply in 2006. (Source: IEA)

The solar energy can be effectively utilized using photovoltaic cells. Photovoltaic cells convert directly the incident solar radiation into electricity, by a clean process, the photovoltaic effect, which produces no pollution or harmful wastes, unlike fossil fuels. The average power from the Sun incidenting on the terrestrial surface is around 1000 W/m^2 and to satisfy the actual energy consumption, it would be necessary to cover around 0,08% of the earth surface with cells assuming an efficiency of ~10%.

In photovoltaic technology, the maximum theoretical efficiency of the single junction solar cell with a 1,5 eV bandgap energy is around 30%. In the case of a solar cell with an infinite number of junctions, the efficiency can be increased up to 60% [13]. This calls for the development of cheaper and efficient solar cells.

The aim of this work is to contribute to the improvement of the efficiency of thin solar cells by increasing the efficiency of light collection in n-i-p structure solar cells based in a transparent layer of aluminum doped zinc oxide (ZnO:Al) thin film. This material has optimum properties to be used as transparent conductive oxide (TCO) contact layer in solar cells, being not as expensive as the traditionally used material. The main goal of the present work was to texturize the as deposited ZnO:Al thin films for light confinement purposes. The texturization was carried out by wet chemical etching with diluted hydrochloric acid (0,5% HCl), a simple and economic method, with which is possible to improve the light trapping in thin film silicon solar cells. Additionally, amorphous silicon (a-Si:H) thin film solar cells were deposited by hot-wire chemical vapor deposition (HWCVD) technique, over the different achieved TCOs, to study the influence of the texturization in the device performance.

This text presents the basics of solar cells and describes the work carried out in detail:

In *chapter2*, the basic principles of solar cells operation and the difference for the thin film solar cells are introduced as well as the parameters used for their characterization. The two configurations for thin film solar cells are compared and the requirements for materials to be used as TCO are also discussed. The theoretical principles of deposition methods to deposit the TCO and the solar cells and the reasons of their choice are explained. Finally, the principles of light trapping by a textured front TCO are also presented.

In *chapter 3* the experimental techniques and procedures followed in this work are explained. After checking the cleaning process, the ZnO:Al films were deposited by r.f.-magnetron sputtering with optimized process conditions. The texturization set-up was developed, the etching conditions were chosen and the films were etched changing some variables on which the resulting surface morphology depends; etching time and substrate orientation. Optical and electrical characterization setups are described. The surface morphology was studied using a scanning electron microscope (SEM) and an

atomic force microscope (AFM). The HWCVD technique for a-Si:H thin film solar cells deposition is presented.

In *chapter 4*, the results obtained from the electrical and optical characterization of the etched films, and also their morphological characteristics are presented. The study of the properties as a function of the etching variables was performed. The results are compared and the performance of a-Si:H solar cells (IV-curve, quantum efficiency, fill factor, open circuit voltage, and short circuit current) are related with the morphology of the TCO. Results obtained with a MATLAB program developed to find out the average period of the textured surface, and how these values are related with the parameters of the solar cells are included.

In *chapter 5*, the conclusions obtained from this work are presented. The proposals for a more deep and complete study on this area is proposed are also suggested.

1. Introduction to solar cells and TCOs

1.1. Solar cells

In 1839, Becquerel discovered the photovoltaic effect, observing that an electric field can be generated between two electrodes attached to a solid or liquid system when illuminated. The modern era of solar cells began in 1954, when the first silicon (Si) solar cell was built at Bell Laboratories, with 6% efficiency.

A simple explanation of the photovoltaic effect is that photons from a source light are absorbed by a semiconducting material and may transfer its energy to the material. The energy is transferred if the energy of the absorbed photon (E_γ) is higher than the difference in energy levels of the valence and conduction band, the bandgap of the material (E_{gap}). When this happens, an electron is excited to the conduction band leaving an empty electronic state in the valence band that acts like a positive particle in the semiconductor, which is designated as a hole. Both electron and hole are charge carriers and participate in the electrical transport. Two other possibilities can take place: the photon can be reflected in the material surface or, when E_γ is lower than E_{gap}, the photon can be transmitted through the material without absorption. The size of E_{gap} determines whether a material is an insulator, a conductor or a semiconductor.

In conductor materials the valence and the conduction band are overlapped, and hence a fraction of the valence electrons can move through the material. Insulator materials are characterized by having large E_{gap} values, and therefore electrons do not move in the material and they do not react to electric fields. A semiconductor has a low enough E_{gap} to allow the thermal excitation of electrons from the valence to the conduction band and is characterized by an electrical conductivity that varies with the temperature and with external electric fields.

According to the type of construction, solar cells are divided into three generations. The first generation is composed by high quality silicon single junction solar cells with large areas and efficiencies approaching the theoretical limit of 30%. These cells are made from the beginning in high quality volume material, leading to low potential for reducing the production costs [1]. In 2007, 89,6% of the solar cell market was first generation [2].

The second generation had its origin when the solar cell industry began to switch to thin film solar cells, in an attempt to reduce the production costs. The most successful and used materials are cadmium telluride, copper indium gallium selenide and amorphous silicon. These materials are deposited as thin films over a substrate, like glass or ceramics, which reduce the use of mass material and consequently reduce the production costs significantly. These cells have lower efficiencies than the ones of the first generation and in 2007 they were 10,4% of the solar cell market.

The third generation appeared as an effort to enhance the second generation cell efficiency keeping the production costs low, and is still a research target and less successful compared to second generation. The key criterion is the use of new materials, like molecularly based organic and dye sensitized cells [1].

1.2. Thin film solar cells

Thin film solar cells are cells composed of several thin layers of semiconducting materials built on a substrate. The thickness of the layers may vary from a few nanometers to tens of micrometers and thus the thin film classification is done in terms of the production process and not in terms of thickness. A good definition is that a thin film is a material produced from the beginning by the random nucleation and growth process of individually condensing/reacting atomic/ionic/molecular species on a substrate [3]. The electrical, structural and optical properties of the thin films depend on the deposition parameters.

A semiconductor can be doped by introducing impurity atoms into the crystal lattice controlling the concentration of electrons and holes: if the atoms introduced in the crystal lattice have one more valence electron than the original atoms, there will be extra electrons and hence a n-type semiconductor is produced; if the doping atoms have one less valence electron than the ones of the crystal lattice, the semiconductor is p-type, because there are extra holes. The Fermi level of an intrinsic (undoped) semiconductor lies near the middle of the bandgap, but when impurities are introduced it varies. In a n-type semiconductor, the Fermi level lies near the conduction band and in a p-type it lies near the valence band, as presented in figure 1.1 and figure 1.2.

A cell is formed when two different type doped material are placed in contact – p-n junction.

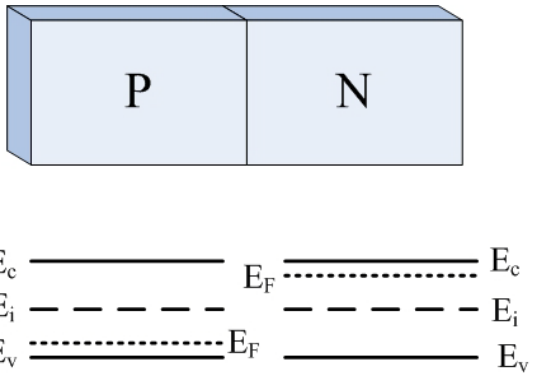

Figure 1.1 Fermi levels of p and n types.

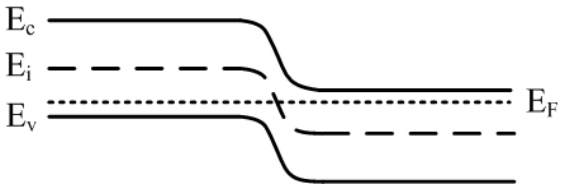

Figure 1.2 Fermi levels adjustment.

In the contact region, electrons diffuse from the n-side to the p-side and simultaneously holes diffuse from p-side to n-side. This movement results in ionized positive and negative impurities fixed in the crystal lattice on the n-type and p-type sides, respectively, and thus an electric field is created across the junction, in a region with no free carriers. This region is called depletion region and, because of the electric field, the holes tend to stay in p-type semiconductor and electrons in the n-type. It can be said that a diode is created, allowing current to pass easily only in one-way.

If a photon enters the depletion zone with enough energy to excite an electron from the valence to conduction band, a pair electron-hole is formed. Due to the electric field in the depletion zone, electrons are swept to the n-layer and holes to the p-layer, and hence a current is produced. The maximum limit value of this current intensity, in the case of junctions used as solar cells, corresponds to all photons of AM 1.5 spectrum[1], with higher energy than the E_{gap} for the semiconductor in use, being absorbed, and all electron-hole pairs generated being collected to contribute to the electric current.

[1] **AM - A**ir **M**ass is the path length which light takes through the atmosphere normalized to the shortest possible path length (Sun is directly overhead). The light produced by the sun is known as AM0 radiation. AM1.5 radiation corresponds to sunlight that has travel 1,5 times the shortest width of the atmosphere, which occurs when the sun's elevation is 48,2 degrees from the horizontal, a fairly typical value for our latitudes.

The equation of the current generated by one solar cell, *I*, is similar to the diode equation and is given by equation (1.1), where I_0 is the saturation current (the leakage current density in the absence of light), I_L is the light generated current, *V* is the applied voltage across the terminals of the diode (cell), *q* is the absolute value of electron charge, *k* the Boltzmann's constant, *T* the temperature of operation of the device and *n* the ideality factor. I_0 is a parameter of the material and depends on E_{gap}.

$$I = I_0 \left(e^{\frac{qV}{nkT}} - 1 \right) - I_L \tag{1.1}$$

I_0 can be determined by the empirical relation, equation (1.2) [3]:

$$I_0 = I_{00} e^{\frac{-E_g}{kT}} \qquad \text{with} \qquad I_{00} = 1{,}5\text{x}10^5 \ (\text{A.cm}^{-2}) \tag{1.2}$$

The I-V curve of a solar cell is a combination of the I-V curve of the solar cell diode in dark with the light generated current. When the light shines in the cell, the I-V curve is shifted because power is generated. The greater the light intensity, the greater the power production and so the shift of the curve will be greater. By convention, it is usual to invert the current axis (figure 1.3) in order to have the integral positive for supplied power.

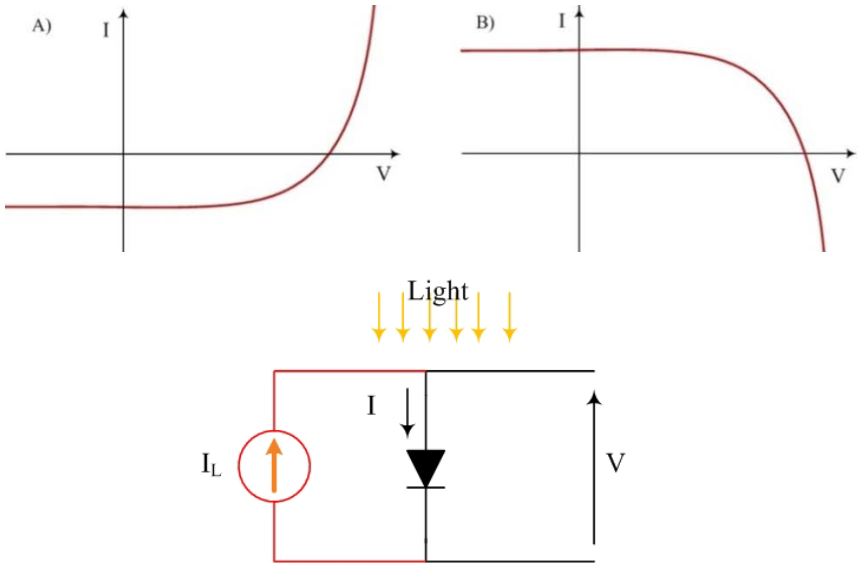

Figure 1.3 Light effect in a typical I-V curve of a solar cell. In figure A) the current axis is not inverted. In figure B), for convention, the current axis is inverted.

The open-circuit voltage (V_{oc}) is the maximum voltage that can be obtained from the cell when illuminated, and this happens when the current through the device is zero. V_{oc} can be calculated with equation (1.3):

$$V_{OC} = \frac{nkT}{q} ln\left(\frac{I_L}{I_0} + 1\right) \quad (1.3)$$

The short-circuit current of a cell (I_{sc}) is the maximum current through the cell and happens when the solar cell is short-circuited, i.e., the voltage across the cell is null (expression (1.4)).

$$I_{sc} = -I_L \quad (1.4)$$

An image of the I-V curve with the open-circuit voltage, V_{oc}, and with the short-circuit current, I_{sc}, is shown below (figure 1.4).

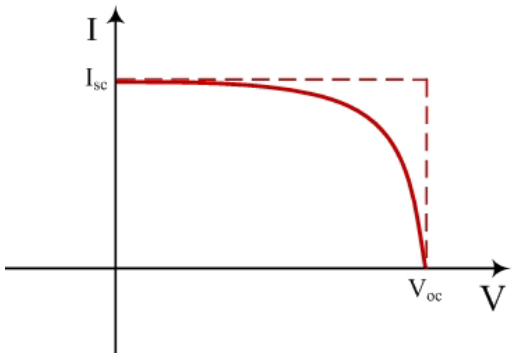

Figure 1.4 I_{sc} and V_{oc} in the I-V curve of a solar cell. (For convention the current axis is inverted).

The fill factor, FF, is related with the form of the I-V curve. It is a parameter that indicates the proximity of the curve to the ideal conditions, and determines the maximum power from a solar cell (figure 1.5). The maximum power of the cell (P_{max}) is given by equation (1.5), and for ideal cells it corresponds to the area of the rectangle in figure 1.4.

$$P_{max} = I_{mp} \text{ x } V_{mp} \quad (1.5)$$

So FF is the ratio between the maximum power and the product of V_{oc} by I_{sc} (equation (1.6)) and for ideal cells FF=1.

$$FF = \frac{I_{mp} \text{ x } V_{mp}}{V_{oc} \text{ x } I_{sc}} \tag{1.6}$$

This corresponds to the ratio of the areas of the shaded rectangles in figure 1.5.

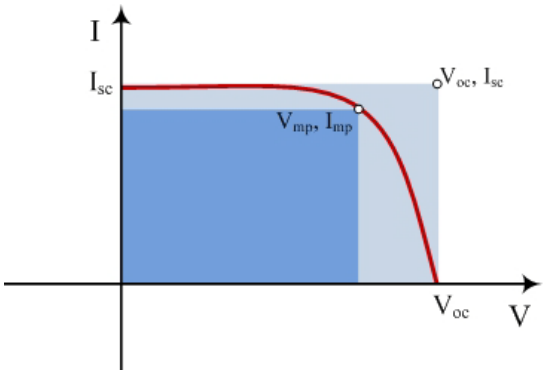

Figure 1.5 I-V curve showing the maximum power point (V_{mp}, I_{mp}). (For convention the current axis is inverted).

The characteristic resistance of a solar cell is the load resistance at which maximum power is supplied (equation (1.7)).

$$R_{ch} = \frac{V_{mp}}{I_{mp}} \tag{1.7}$$

The cell efficiency, η, is obtained dividing P_{max} by the incident power, P_{inc}, and gives us the fraction of incident power which is converted into electricity (equation (1.8)).

$$\eta = \frac{P_{max}}{P_{inc}} \tag{1.8}$$

This equation can be written as (equation (1.9)):

$$\eta(\%) = \frac{V_{oc} \times I_{sc} \times FF}{P_{inc}} \times 100. \tag{1.9}$$

Parasitic resistances reduce the solar cell efficiency by dissipating power, and the most common are designated as series and shunt resistances. With the I-V curve under illumination it is possible to take information about these resistances because they affect the curve in different regions. In figure 1.6 are represented the referred influences of the resistances.

The series resistance (R_s) is the resistance of the cell material to current flow and has its cause in the movement of current through the front surface to the contacts and from resistive contacts. This does not affect the open-circuit voltage but strongly affects the I-V curve near it and also reduces the short-circuit current, reducing the fill factor.

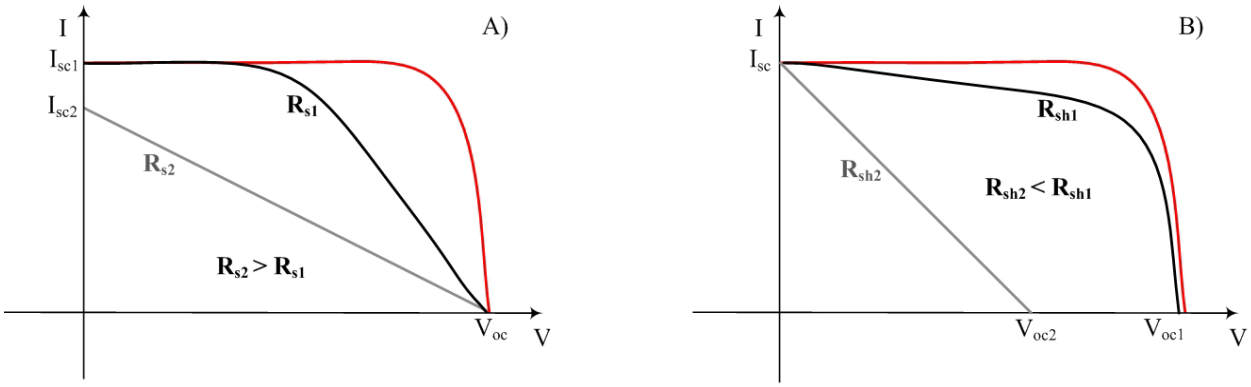

Figure 1.6 Effect of parasitic resistances in I-V curve. In image A) is represented the effect of different values of series resistances (R_s). In image B) is shown the effect of different values of shunt resistances (R_{sh}).

The shunt or parallel resistance (R_{sh}) is typically due manufacturing defects. Low R_{sh} gives rise to leakage current through the cell, because provides an alternate path for the light-generated current, and has no effect in the short-circuit current, but the I-V curve near it is affected and reduces the open-circuit voltage. A typical equivalent circuit of a solar cell is shown in figure 1.7.

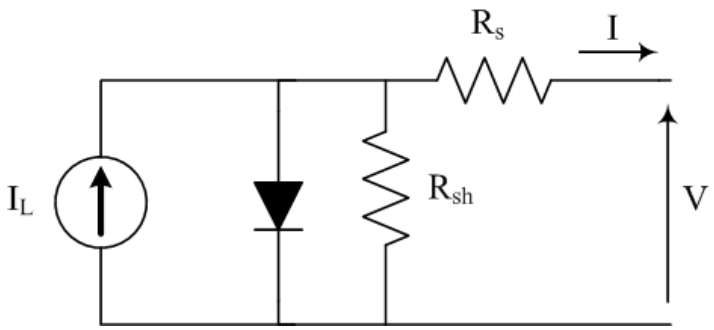

Figure 1.7 Equivalent circuit of a solar cell.

The dark I-V curve of a solar cell is the characteristic I-V curve of the cell under no illumination. It is obtained by applying a voltage to the cell, V, i.e., by injecting carriers into the cell instead using the light generated carriers. The I-V characteristic curve essentially corresponds to the curve of a normal diode (figure 1.8), showing that in dark a solar cell is simply a diode.

With a semilog graph of the curve, it is possible to extract more information about the diode properties and it also shows how a device operates as a p-n junction and can be used to determine the influence of the shunt and series resistances. It is also possible to calculate the saturation current, I_0, and have a measure of the recombination rate in the cell: the higher $I_{0,}$ the higher the recombination velocity.

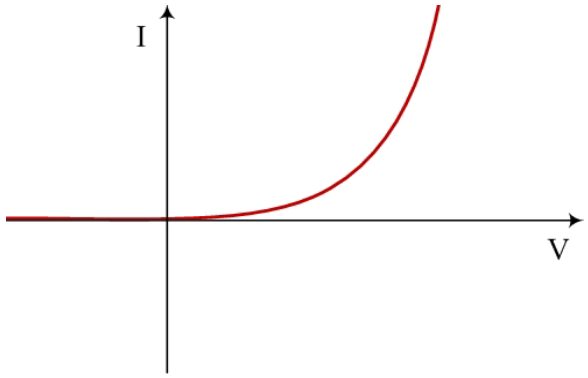

Figure 1.8 Dark I-V curve of a solar cell. The curve corresponds to the curve of a normal diode.

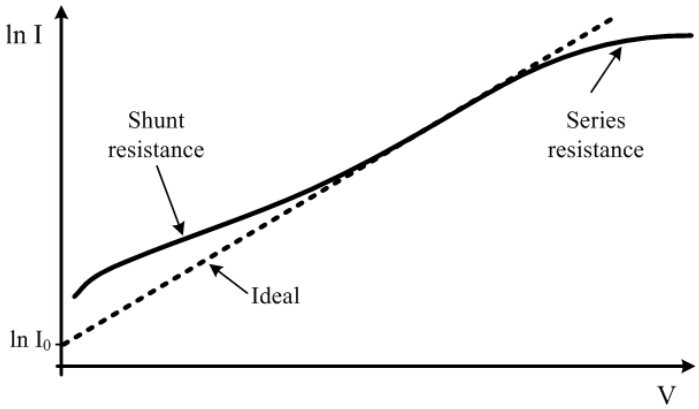

Figure 1.9 Semilog plot of the dark I-V characteristic of an ideal and non ideal solar cell. The series and shunt resistances affect different regions of the curve.

In figure 1.9 are presented the semilog plot of the dark I-V curves of an ideal cell and of a non-ideal cell. The ideal cell curve is linear, since the I-V curve of an ideal cell is exponential. However, the non-ideal curve shows different regions dominated by different loss mechanisms.

The effect of leakage currents is directed related with low I region of the curve, while the series resistance is related with high current values. The asymptotic current value for zero voltage in the dashed curve gives the saturation current, I_0.

Another parameter that characterizes a solar cell is the external quantum efficiency, EQE, i.e., the ratio of the number of carriers collected by the solar cell to the number of photons of a given energy incident on the solar cell. This parameter depends on the absorption coefficient of the cell material, the efficiency of charge separation and the efficiency of charge collection.

In figure 1.10 it can be seen the EQE of a real solar cell compared with an ideal one: in zone a) there is a reduction of the EQE due the front surface recombinations in the cell; in zone b) the reduction is due the reflected photons and low diffusion length of the carriers on the cell; zone c) suffers an EQE reduction due rear surface passivation, reduced absorption for long wavelengths and also due low diffusion lengths. The EQE is zero at long wavelengths because no light with energy below the bandgap is absorbed.

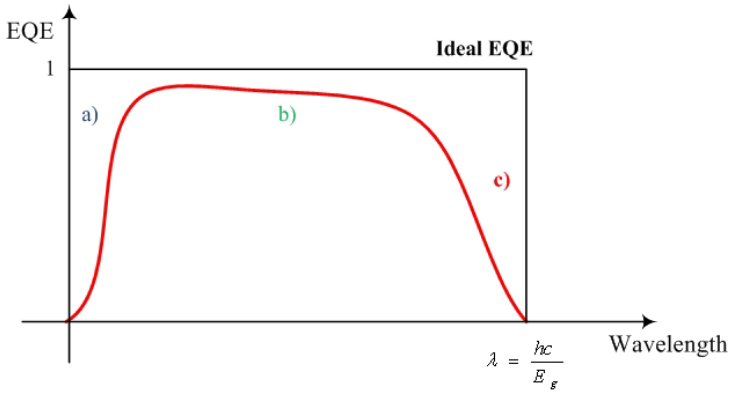

Figure 1.10 External quantum efficiency of a real and an ideal solar cell. There is a reduction of EQE at zones a), b) and c) due different loss processes.

While the optical losses of the device, such as transmission and reflection, are inherent to the external quantum efficiency, the internal quantum efficiency, IQE, refers to photons that are not reflected or transmitted out of the cell, and generate collectable carriers.

1.2.1. Si thin film solar cells

The semiconductors to be used in thin film solar cells should fulfill the following requisites:

- Have a band gap between 1-1,5 eV;
- High solar absorption between 350-1000 nm;
- High quantum yield to the excited carriers;
- Diffusion length of the carriers should be long;
- Low recombination velocity. [3]

Actually the most used semiconductor in solar cells applications (more than 95%) is silicon, Si, due its natural abundance (about 15% of the composition of earth mass) and consequent low cost (figure 1.11). The micro crystalline silicon, μc-Si, has an indirect gap of 1.12 eV, and hence the sunlight is very efficiently absorbed [4]. Because this gap is indirect, to absorb a significant amount of sunlight a film of Si should have a thickness greater than 700 μm [5]. This large thickness implies longer production times and very high production costs. Another disadvantage is that an increased thickness reduces the collection of carriers since the diffusion length of the carriers is in general smaller.

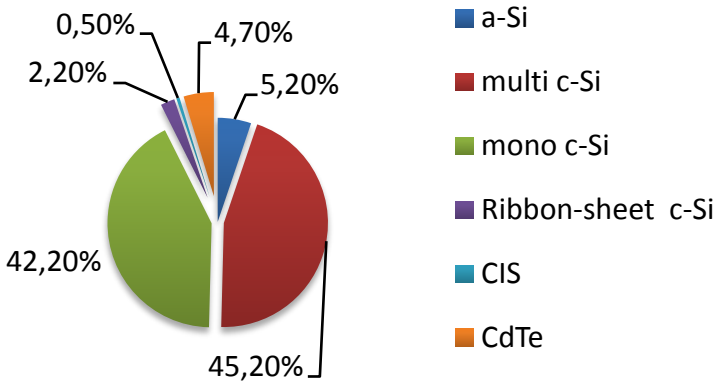

Figure 1.11 Cell technology shares in 2007 (source: EPIA).

Because the absorption coefficient of the Si is low when the energy of the incoming light approaches the E_{gap} of the material, a Si thin film solar cell efficiency is also low for the corresponding wavelengths and gets worse when the thickness is reduced. One way to enhance the absorption and consequently the efficiency, is to

increase the optical path length to several times the actual device thickness with a consequent increase of the absorption probability of the photons in the cell (the optical path length of a device refers to the distance that an unabsorbed photon may travel within the device before it escapes out of the device). This can be achieved by trapping the light in the cell, using multireflections within the Si wafer and also by texturizing the transparent conducting oxide (TCO) covering the wafer. The detailed discussion of light trapping is present in Chapter 1.5.1.

The semiconductor used in the solar cells can be amorphous silicon (a-Si), or microcrystalline silicon (μc-Si). The main differences of μc-Si relatively to a-Si are: drastic dependence with the deposition condition and an increased sensitivity to layer contamination; μc-Si has an E_{gap} of 1,1 eV while a-Si has 1,8 eV; this confers to μc-Si a higher absorption in the near infrared region (figure 1.12). Microcrystalline solar cells have efficiencies 9 to 10%, and the best way of using μc-Si is in micromorph tandem cell, which is a combination of a μc-Si cell as a bottom cell with an a-Si solar cell on the top to increase the blue light absorption. This tandem cells efficiency, when stabilized, is between 11%-12% [5]. The most important advantage of a-Si relating to μc-Si in large scale production is its fabrication cost, because a-Si layers can be thinner than μc-Si and hence less material is used. Other advantages are:

- Better absorption under non-direct or weak light conditions;
- Less sensitive to temperature, so have a better performance under high insulation than μc-Si.

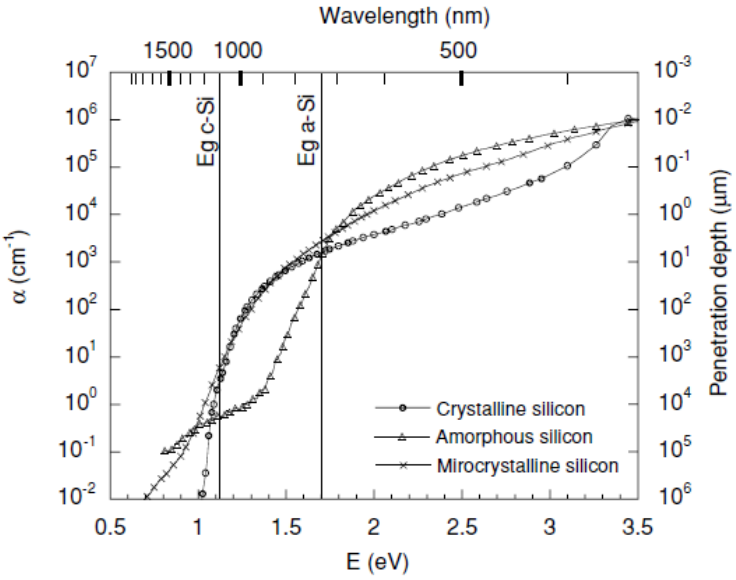

Figure 1.12 Optical absorption spectrum of μc-Si, a-Si and c-Si. [6]

The transparent conducting oxide (TCO) is used as a front contact in thin film solar cells based on amorphous or microcrystalline silicon, and the chosen TCO material must fulfill some requirements for the sake of the good device performance. It acts both as an ohmic contact to transport the carriers out of the device and as a window for light entering the cell. Also, when textured, it has light confinement properties.

1.2.2. p-i-n and n-i-p configurations

An improvement to thin film solar cells is the introduction of an intrinsic layer between p and n regions.

There are two possible configurations for thin film solar cells composed by n, p and intrinsic layers: p-i-n and n-i-p structures (figure 1.13). The great advantage and difference of these configurations to the p-n junction solar cells is the presence of an intrinsic layer. In p-n cells, when the electron-hole pair generation (photon absorption) occurs outside the depletion region, the carriers slowly diffuse towards the depletion region and a significant part of them recombine before reaching it. The ones that reach the depleted area are swept away across the junction to produce an external electrical current. In a p-n junction the depletion region is a small portion of the total device volume and most of the carriers' generation occurs outside it, implying that the carriers have highly recombined before reaching the depletion region. Also, because of the slow movement towards this region, the current is delayed with respect to photon absorption.

To overcome the recombination problem, the depletion region is increased placing an intrinsic material layer between the p and n doped layers. Because the i-layer has no free carriers, its electrical resistance is high and the potential difference created in p-i and i-n junctions imply strong electrical forces within the i-region that artificially extends the depletion region to a significant fraction of the total solar cell thickness. This means that in these case, most of the photons are absorbed within the depletion region, the generated carriers being immediately swept away by the electric field to the n or p layer, suffering no recombination as in p-n junction case. The higher the i-layer thickness, the higher the probability of photons to be absorbed within it [18]. On the other hand, the field-enhanced collection compensates the short lifetime of the carriers, allowing amorphous silicon to be used in solar cells.

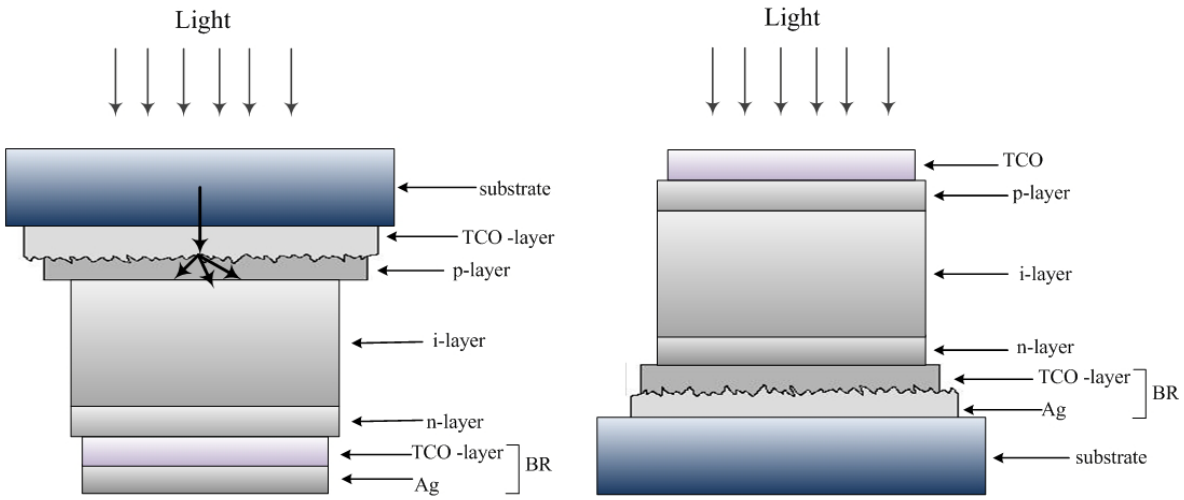

Figure 1.13 Si thin film solar cell configurations: at the left side is a p-i-n structured solar cell and in the right side a n-i-p solar cell.

The p-i-n configuration is a superstrate[2] design. The characteristics of this configuration are:

- The light enters through the substrate, which is a transparent layer like glass or plastic;
- Because the substrate materials are insulators, it is necessary to deposit a transparent conductive oxide over it;
- The silicon layers are then deposited in p, i and n-layer order over the substrate;
- Finally the back reflector is deposited at the end.

The n-i-p structure is a substrate design and its characteristics are:

- The substrate does not need to be transparent;
- The back reflector is first deposited onto the substrate;
- Then the Si layers are deposited over it in n, i and p-layer order;
- Finally the TCO is deposited behaving as the window for the sunlight to enter into the cell.

So, the main difference between the two configurations is that in the p-i-n structure the sunlight enters by the transparent substrate (a glass or a transparent plastic)

[2] The glass substrate acts both as support and window for light entering the cell.

and in the n-i-p by the TCO. Typically, the p-layer has a thickness around 20 nm, i-layer a few hundred nanometers and the n-layer around 30 nm.

Because the p-layer is an almost transparent layer, the most part of the photons are absorbed in the thick i-layer. The large i-layer is inside the depletion region and most of the electrons and holes are produced in this region and swept away to the n-layer and p-layer [5]. Because the holes are collected in the p-layer and have mobilities smaller than the ones of the electrons, the entering of the sunlight is performed through the p-layer.

1.3. Transparent Conducting Oxides used in Si thin film solar cells

A transparent conducting oxide (TCO) material has to be a transparent window (over the spectral region the solar cell is operating) to the cell, to minimize optical losses, and to have low electrical resistance, so the cell series resistance is low. To be transparent, usually a material has to have a bandgap greater than 3 eV so the near UV radiation, around 0.41 μm, can be transmitted to the cell. The material should also have its free carrier plasma resonance absorption in the near-infrared (1.5 μm) or longer wavelengths [7].

The TCO layer has important roles in a solar cell performance: it is a conducting layer over the insulating substrate and, when textured, facilitates the optical confinement. Among the different TCO materials, fluorine doped tin oxide (SnO_2:F), aluminum doped zinc oxide (ZnO:Al) and indium tin oxide (ITO) are the widely used ones in the Si thin film solar cells. The most used is tin doped indium oxide (ITO), because it is the one that best fits the requirements [7].

The most usual commercial TCO substrate is the Asahi-U, which consists in a rough layer of tin oxide doped with fluorine, SnO_2:F, deposited by atmospheric pressure chemical vapour deposition (APCVD) over a glass. With this technique, films with a rough surface with optical interests are produced, since the roughness of the film is random and has a rms roughness around 35 nm, which is a good value to deposit amorphous silicon solar cells to scatter the light at the front contact [4].

Recently ZnO thin films have found much application as the front TCO in Si thin film solar cells, since a textured growth of ZnO is possible by metal organic chemical vapour deposition (MOCVD) technique.

1.3.1. ZnO:Al thin films

The high cost and disposability issues of Indium makes necessary to find other TCOs that fulfill the requirements and zinc oxide (ZnO) is one of the alternatives. Although it is not as good as ITO, it is abundant and its costs are lower. Undoped ZnO has a high electrical resistance but it is easy to dope with aluminum (Al), or gallium (Ga) or boron (B) to form good degenerate transparent conducting oxides. ZnO:Al and ZnO:Ga are generally deposited by sputtering technique while the ZnO:B is deposited by MOCVD [12]. One of the advantages of MOCVD grown ZnO is that it will grow with its natural pyramidal texture. This textured ZnO:B can be used as the front transparent contact for the p-i-n type Si thin film solar cells. Other application of doped ZnO thin films in the Si thin film solar cells is in the back reflector stack along with a metallic reflector (Al or Ag).

In figure 1.14 a typical total transmittance spectrum of aluminum doped zinc oxide (ZnO:Al) is represented. Observing the spectrum, it can be noticed that transmittance is zero for 330 nm, which corresponds to a ZnO:Al bandgap energy of ~ 3,8 eV.

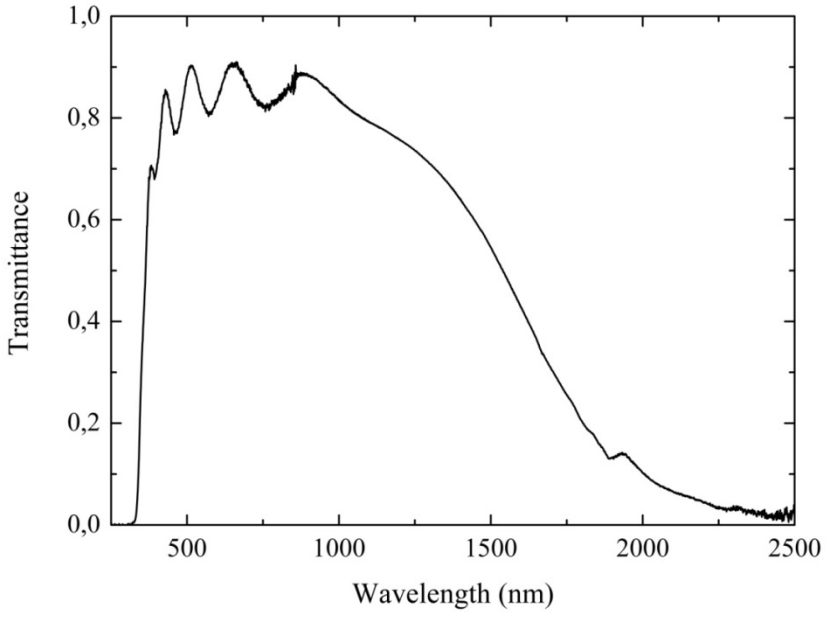

Figure 1.14 Typical transmittance spectrum of an r.f. magnetron sputtered ZnO:Al thin film.

1.3.2. Light trapping in Si thin film solar cells

The texturized TCO layer traps light due to the surface topography and also leads to a decrease of reflected light, because a part of the light is reflected back to the cell (see figure 1.15). In this way, it is possible to get an increase in the short circuit current and an increase of the cell efficiency (mainly for long wavelengths, that corresponds to low absorption coefficients and with the increased path length the absorption probability increases).

The Si and ZnO:Al refraction indices are different, the Si index being higher than the ZnO:Al and hence the light is refracted at the interface. An ideal rough surface must have a pyramidal shape so the incoming light can be refracted into angles that are larger than the critical angle for total reflection in silicon. The light is then trapped within the Si absorber layer (figure 1.15). However the pyramids should not be too sharp because the incidence angle in Si would be too small and the light will not be efficiently captured.

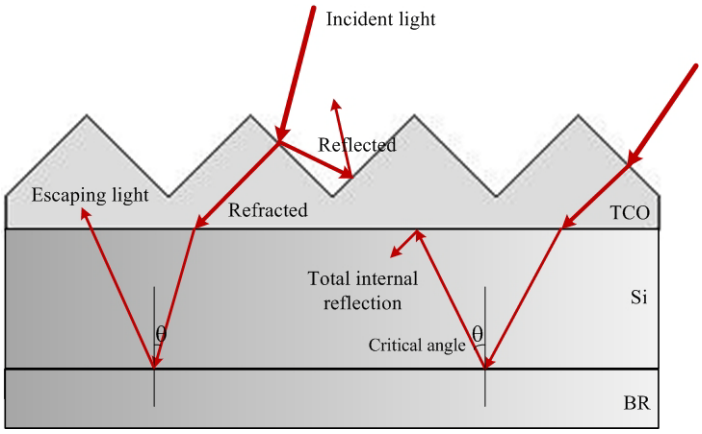

Figure 1.15 Solar cell scheme with textured TCO. Light reflected by angles above the critical angle are totally reflected.

A way to achieve r.f. magnetron sputtered films with surfaces presenting a pyramidal like roughness is to etch them with hydrochloridric acid (HCl). With this technique is possible to give different roughness types, by changing some parameters.

Usually, to characterize a rough surface, the used parameters are: the roughness rms, which is a statistical measurement of the roughness magnitude; the haze, which is

the ratio between the diffuse and total transmittance and is defined as the portion of light incident on a film that is scattered incoherently; the angular resolved scattering that is a measurement of the scattered light intensity in several solid angles. The different textured ZnO:Al films were used to deposit amorphous silicon thin film solar cells by hot-wire CVD .

2. Experimental and Analytical Techniques

In this chapter all the processes and steps of the deposition of the ZnO:Al and its chemical wet etching are described, as well the hot wire chemical vapour deposition of amorphous Si thin film solar. All the used set-ups are presented and the optical, electrical and morphological characterization methods are explained.

2.1. Substrate Cleaning

Corning 1737F glass of 5,0 x 5,0 cm^2 area with 1,10 mm of thickness was used as the substrate. The cleaning process of the substrate is a very important step because the thin film growth quality depends on the adhesion and the surface cleanliness, so the substrate must be as clean as possible.

The initial cleaning process was a simple one, carried out by cleaning the glass with isopropanol (IPA) followed by acetone. Then the process was ended by drying the substrate with blowing nitrogen. After this process, stains on the glass surface were observed, and for this reason a new cleaning process was developed. The applied concepts on the new cleaning process are described below.

The most important variables in cleaning, using aqueous methods are [14]:

- Precleaning handling;
- Cleaner;
- Agitation;
- Temperature;
- Cleaning time;
- Rinse used;
- Drying method;
- Postcleaning handling.

As precleaning condition of the glass substrates, these were stored in protective packages, avoiding them to be exposed to the dusts present in the surrounding atmosphere. The cleaning steps were performed in the Clean Room of Universitat de Barcelona, following the protocol present in Appendix A. Before starting the cleaning

processes, the glasses were cleaned with blowing nitrogen, in order to physically remove the dust deposited on the surface.

The cleaning process can be resumed by the following steps:

- Immersion of the substrate in a diluted DECON 90 detergent in deionized water (Millipore Q-POD) in a proportion of 1:4, and manually cleaning with a soft brush. With this, the dust that remained on the surface and the grasses that could be on it were removed;
- Drying with blowing nitrogen and cleaning with DECON 90 detergent in an ultrasonic immersion tank for 5 minutes;
- Rinsing the glass with deionized running water for complete soil and detergent removal;
- Glass drying with blowing nitrogen;
- Cleaning with acetone in the ultrasonic bath for 5 minutes;
- Immersion of the substrate in deionized water immediately after the acetone cleaning, because water is the last thing that should touch the surface [14];
- Finally the water was physically removed by blowing nitrogen over it.

Looking at the substrates with naked eye, it was possible to see that there were no dusts or stains on the surface. After these steps the glasses were stored on clean plastic boxes to prevent dusts to deposit on the surface while transporting to the deposition chamber for the ZnO:Al deposition.

2.2. ZnO:Al deposition by r.f. magnetron sputtering

The ZnO:Al films used in this work were deposited by radio-frequency magnetron sputtering (r.f. magnetron sputtering). This is a Physical Vapour Deposition (PVD) technique used to produce thin films of a wide range of materials, and can be understood as the ejection of material from a source (the target) onto a substrate. The target and the substrate are mounted in a vacuum chamber, facing each other, and there are magnetrons behind the target (thus the name of the technique).

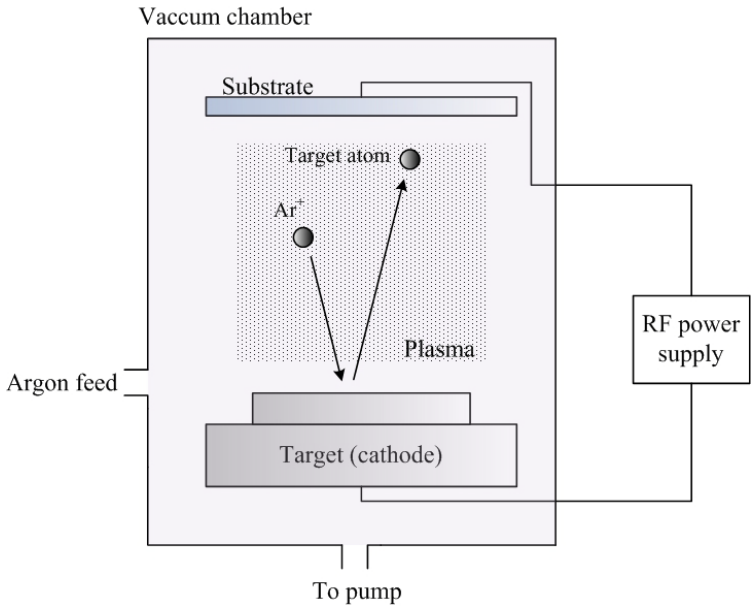

Figure 2.1 Scheme of a sputtering system and some of its components.

The first step to sputter a material is to achieve good vacuum, with a base pressure of typical values from 10^{-6} to 10^{-10} Torr. Then a controlled and continuous flow of an inert gas, such as argon (Ar), is introduced in the evacuated chamber until a pressure from 1 to 100 mTorr is established. When power is supplied to the magnetrons and a negative potential is applied to the target (cathode), while the substrate is grounded, a plasma is produced. The plasma is formed due to the ionization of the Ar gas. With the potential difference, the free electrons are accelerated and collide with the gas atoms, ionizing the Ar atoms and producing more electrons to continue the process (figure 2.1). The Ar ions are attracted towards the target surface and collide with it releasing atoms from the target surface. This process is called sputtering. Since these atoms are neutrally charged, they are not affected by the magnetic field and travel to the substrate and collide with it, forming the thin film coating.

When an Ar ion collides with the target surface, the emission of electrons also occurs. The emitted electrons become trapped in the magnetic field produced by the magnetrons, following helical paths around the magnetic field lines contributing to additional collisions between electrons and neutral atoms and the production of more positive ions. These ions are attracted towards the target and the sputtering process is repeated. The trapped electrons form an increased ion density zone near the target implying a high deposition rate and less electrons reaching the substrate. The use of the

radio frequency allows the sputtering of insulating materials at a practical rate [8]. Using r.f. the electrodes where the target and the substrate are placed reverse roles on each half cycle. The discharge rate is high enough to avoid charge accumulation in the electrode that is serving as a cathode [9].

The deposition of the transparent conductive oxide was performed in a commercial sputtering system, ATC ORION Sputtering System of the Aja International Inc. (figure 2.2). The system is equipped three magnetron targets each of capable of holding 3 inch targets. The substrate can be rotated with the rotating feedthrough assembly at 20 rpm and a maximum substrate temperature of 800 ºC can be achieved by radiation heating using halogen lamps. A cross section of the chamber is shown in figure 2.3.

Figure 2.2 Aja International sputtering system.

In this work, a ZnO:Al (ZnO doped with 2 wt% Al_2O_3) sputtering target of 3 inches in diameter and 99,995% purity was used. The distance between the target and the substrate (T-S) can be changed within a range of 11 to 18 cm. The substrate heating is carried out by radiative heating from halogen lamps.

Four 5,0 x 5,0 cm^2 glass substrates were used for the deposition at a time, making a square of total area 10 x 10 cm^2. The deposition of ZnO:Al was carried out with a substrate rotation of 10 rpm to achieve a better homogeneity.

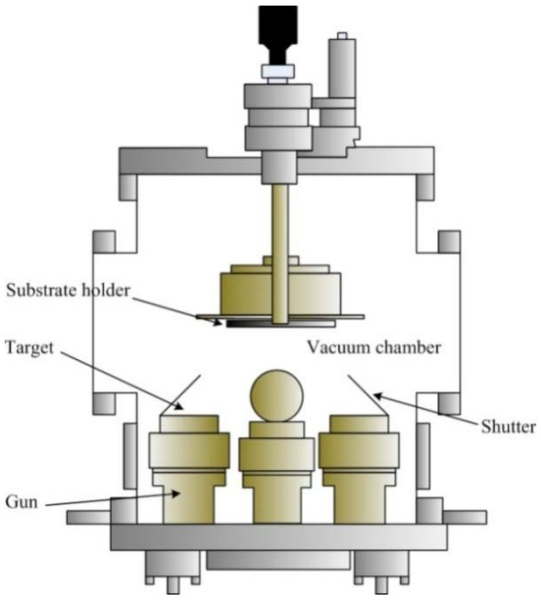

Figure 2.3 Cross section of a sputtering chamber.

The shutter position (open/closed) determines whether the deposition begins/ends: if the shutter is closed no sputtered atoms are able to reach the substrate.

By previous studies, it was observed that the resistance of the r.f. sputtered films against wet chemical etching with diluted HCl strongly depends on the deposition pressure and is influenced by the deposition temperature. The range of deposition pressures to obtain ZnO:Al film that can be used for etching purposes to produce textured surfaces for light trapping, was determined to be 1 to 5 mTorr [15]. The films deposited at pressures lower than this range, gave very low roughness and were not good for light trapping after etching; whereas for the values above this range, the obtained texture has very sharp pyramids and the incident light is not efficiently captured.

The deposition pressure was selected based on this fact and other previous studies, which show that for this pressure range and 200W of applied r.f. power on the target, the obtained ZnO:Al thin film has good electrical and optical properties. The deposition conditions were the same for all the samples and are shown in table 2.1. The system was pumped down to a base vacuum of $4x10^{-6}$Torr. The substrate temperature was kept at 350 ºC. The deposition was carried out with an Ar gas flow of 12sccm[3] and at an r.f. power of 200W.Under these conditions the obtained films are polycrystalline.

[3] Sccm is a flow measurement term and stands for Standard Cubic Centimeters per Minute.

Table 2.1 Deposition conditions of ZnO:Al sputtered films.

Base Pressure	Dep.Pressure	Ar flow	Power	Substrate Temp	T-S dist	Duration (min)
~ $4x10^{-6}$ Torr	3 mTorr	12 sccm	200 W	350 ºC	15	125

A pre sputtering of 3 min was done to eliminate the possible absorbed gases on the target surface. The sputtering time was based on previous depositions with the same conditions where the deposition rate was estimated. The sputtering was carried out to achieve a film thickness of ~700 nm.

2.3. Wet-chemical etching of sputtered ZnO:Al thin films

The texturization of the ZnO:Al film was performed by wet-chemical etching at room temperature (~28ºC), which changes the flat film surface to a random textured one. Prior to etching, the 5,0 x 5,0 cm^2 deposited samples were cut into half, so the etched samples were with an area around 5 x 2,5 cm^2.

The chemical etching was carried out using 0,5 wt% diluted hydrochloric acid (HCl in deionized water). This acid concentration is regarded to be the best for etching sputtered ZnO films since a strong acid etching of this material would be uncontrollable [16]. The sample to be etched was immersed in a precipitation vessel with dilute HCl acid. A magnetic stirrer (Jenway 1000) was used to agitate the solution. The sample was held at the middle of the vessel using plastic clamps and could be vertically or horizontally oriented. In the horizontal case the film surface is kept downwards (figure 2.4). During the etching it is very important to avoid air bubbles from sticking to the film surface, because they will protect the film from the acid and there can be spots of flat film. This effect is more critical in the case of horizontal etching. In order to solve this issue, during the etching process soft circular movements were performed, so that air bubbles could be released from the surface.

The beginning of the etching time was considered as the moment the entire sample was immersed and the end when it was entirely removed from the acid. Next to the precipitation vessel containing the acid, there were two vessels with deionized water. After the defined etching time was over, the sample was immediately immersed in the first water vessel (the transfer took less than 1 second from the acid to the water

vessel) while performing circular movements, to remove the acid traces from the sample.

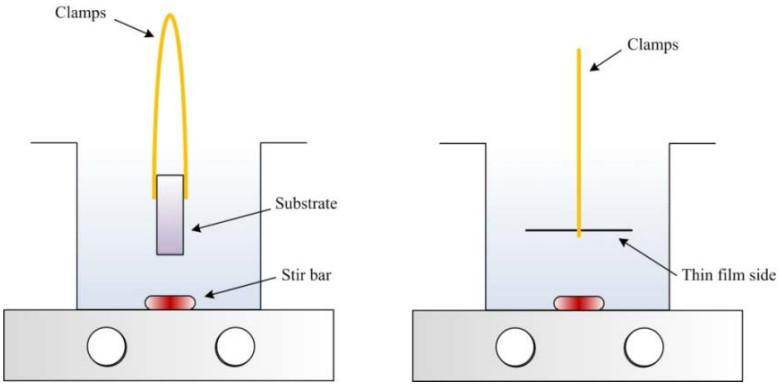

Figure 2.4 Schematics of ZnO:Al etching. In the left side the picture shows the vertical orientation and the one on the right is a side view of the horizontal orientation etching.

After few seconds rinsing in the first vessel, the sample was moved to the second one, and again rinsed to and then placed in a holder to keep it vertically in the water as shown in figure 2.5. The point of having two vessels of water is to guarantee that no acid is left in the film surface that would continue corroding it, so the films can be stable after the etching.

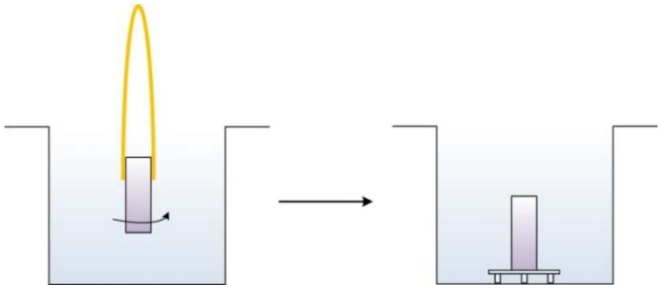

Figure 2.5 Water vessels scheme for acid removal.

After the whole chemical etching process, the samples were dried with blowing nitrogen and placed in plastic clean boxes. The etching conditions for the different films used for cell deposition are shown in Table 2.2.

Table 2.2 Etching times for the samples applied in solar cells.

	S1	**S2**	**S3**	**S4**
Etching time (s)	15	20	10	20
Orientation	horizontal	vertical	horizontal	horizontal

2.4. Hot Wire Chemical Vapour Deposition

The Hot Wire Chemical Vapour Deposition (HWCVD) is a chemical route to produce thin films. The HWCVD technique was used to deposit the p-i-n type a-Si:H solar cells. The basic principle of HWCVD is as follows. The substrate is mounted in a vacuum chamber, over a filament. Then, reactant gases are introduced into the evacuated chamber and the deposition takes place by catalytic decomposition of those gases at the surface of the resistively heated filament (1500 - 2000ºC).

To deposit the intrinsic layer of the cell of hydrogenated amorphous silicon (a-Si:H), a mixture of silane (SiH_4) and hydrogen (H_2) gases were used. The gas molecules are chemically decomposed by a catalytic process when they strike the heated filament. After the catalytic dissociation, mainly atomic hydrogen (H) and atomic silicon (Si) are released from the process taking place at the filament surface (figure 2.6) [10]. Some of these atoms suffer secondary reactions as they diffuse to the substrate, giving origin to radicals, as SiH_2, SiH_3, Si_2H_4, etc. The H and Si atoms that did not suffer any collision and the silicon radicals will reach the surface of the substrate and form the silicon thin film.

The films can be either amorphous or microcrystalline, based on the dilution of hydrogen used and also on the substrate and filament temperature. The doped layers are deposited by using dopant gases along with silane and hydrogen. Phosphine (PH_3) and trimethyl boron($(CH_3)_3B$) are used as the dopant gases for the n-type and p-type layer, respectively. After dissociation some atoms reach the substrate without suffering any collision, while others participate in secondary reactions before reaching the substrate.

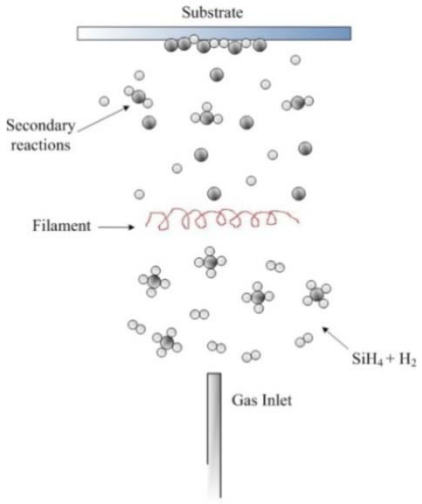

Figure 2.6 Schematic representation of the process of HWCVD technique.

Besides the geometrical dependence of the properties of the deposited film (distance between the filament and the substrate) it also depends strongly on the state of the filament (reason why it is crucial to clean it between depositions) and on the secondary reactions of the gas molecules during the deposition. Other parameters are also important, such as the substrate temperature, which influences the mobility of the radicals in the substrate surface, and also the deposition pressure, filament temperature, filament surface area and proportions of the gases.

The most important advantages of this deposition technique relatively to other techniques are:

- The higher deposition rate;
- Lack of ion bombardment;
- Greater ability to produce atomic hydrogen;
- Great stability;
- Low cost equipment and maintenance;
- Easy to deposit in large areas. [10,11]

2.4.1. The HWCVD set up

The used HWCVD system consists in three inline ultra-high vacuum chambers isolated from each other by gate valves. With this configuration it is possible to produce a solar cell without exposing the device to the atmosphere between the deposition of the different semiconducting layers, minimizing the oxidation and contamination from the atmosphere. The substrate is moved from chamber to chamber with a magnetic transfer system. An overview of the system and a cross section of a deposition chamber are presented in figure 2.7 and figure 2.8, respectively.

Two of the chambers are used to deposit the layers, while the other chamber is used as a load-lock chamber. Of the two deposition chambers, one is used to deposit the intrinsic layer and the other one is used to deposit the doped layers, in way it avoids the cross contaminations in the intrinsic layer. The contamination of the i-layer would be crucial, because this would become unsuitable to be used in photovoltaic devices.

The deposition pressure is controlled by changing the pumping section of the turbo pump with the butterfly valve, and uniform heating of the substrate is obtained with a resistive heater. In the case of intrinsic layer deposition, an external heater was used to avoid the possible contaminations.

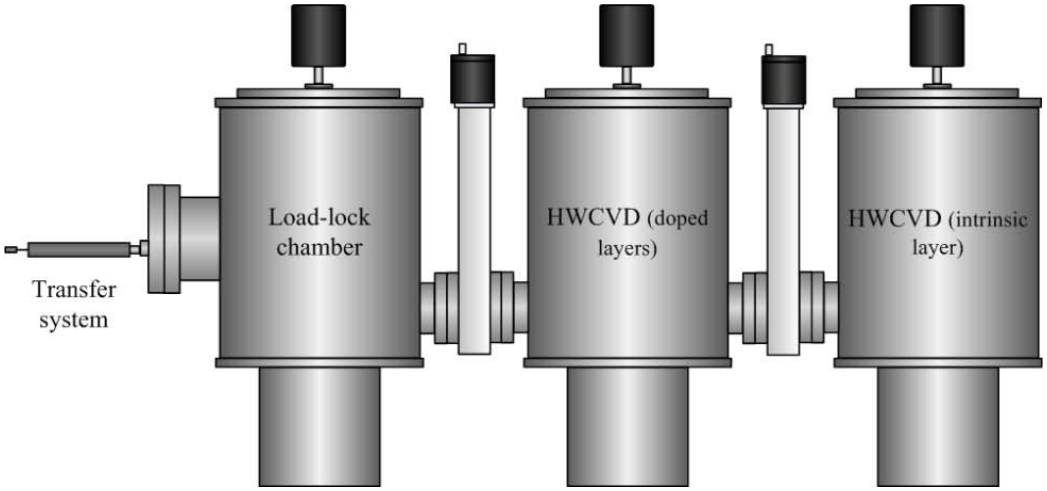

Figure 2.7 Overview of the HWCVD used system.

The best wire configuration for the filament is two parallel filaments, because it gives the deposited film a better homogeneity than a single linear filament. Two tungsten (W) filaments were mounted separated by a distance of 3 cm from each other, and a homogeneous growth of the film along the substrate may be obtained. The distance between the substrate and the filaments is 4 cm.

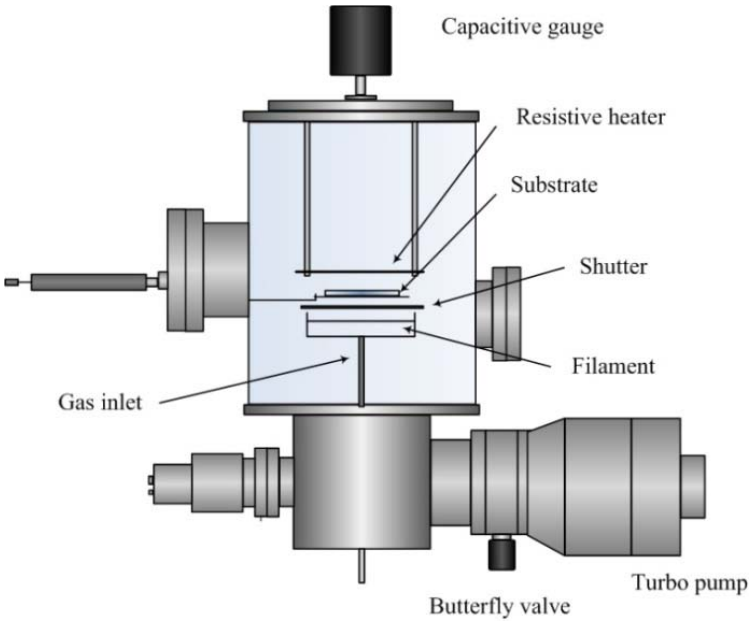

Figure 2.8 Cross section of a HWCVD deposition chamber.

2.4.2. Deposition of a-Si:H solar cells

All the textured ZnO:Al films deposited as discussed in section 2.2 were cleaned with acetone in an ultrasonic bath and rinsed with deionized water and dried with blowing nitrogen before the cell deposition.

The deposition conditions of the intrinsic and doped layers are resumed in table 2.3. In the table, T_s is the substrate temperature, T_w is the wall temperature of the reactor, P the pressure of the used gases, $t_{pre\text{-}dep}$ and t_{dep} the pre-deposition and the deposition times, respectively, $I_{filament}$ the current through the filament and the used gases flows are also presented.

Table 2.3 Deposition conditions of the p, i and n-layers of the HWCVD deposited cells.

							Gas flow (sccm)			
Doping	**T_s (ºC)**	**T_w (ºC)**	**P (mbar)**	**$t_{pre\text{-}dep}$ (min)**	**t_{dep} (min)**	**$I_{filament}$ (A)**	**H_2**	**SiH_4**	**PH_3**	**TMB**
p-layer	140	100	$2x10^{-2}$	7	3	12,5	32,8	3	-	10
i-layer 1	200	100	$1x10^{-2}$	6	0,25	12,5	-	4	-	-
i-layer 2	200	100	$3x10^{-2}$	-	15	10,5	18	4,5	-	-
n-layer 1	120	70	$5x10^{-3}$	2	1	12,9	-	-	2	-
n-layer 2	120	70	$1x10^{-2}$	-	3	12,9	15	-	2	-

The p-layer is μc-Si:H and was obtained with the precursor gases hydrogen (H_2) silane (SiH_4) and trimethyl boron ($(CH_3)_3B$). Trimethyl gas is diluted by 2% in hydrogen. The n-layer was deposited using the dopant gas phosphine. The phosphine gas used was diluted 5% in silane.

To deposit the a-Si:H i-layer, SiH_4 and H_2 were used. This layer was deposited in two steps: a very thin intrinsic amorphous buffer layer was deposited using only SiH_4 gas, under the conditions presented in table 2.3; in the second step the shutter was closed to stop the deposition and the conditions were changed. H_2 was then inserted in the chamber and the active intrinsic a-Si:H film was deposited.

Finally, the n-layer was also deposited in two steps. The deposition pressure was adjusted with the hydrogen and phosphine in the chamber. Hydrogen was closed and the deposition was done only with phosphine for a specific time. Then, the shutter was

closed and hydrogen was introduced again in the chamber. After the pressure values were stabilized the shutter was opened to continue the deposition.

After each deposition, the filaments of the used chambers were cleaned to remove any material deposited in it. The cleaning process is made by heating the filament with a current of 14 A (which corresponds to a temperature around 2000 ºC) and introducing 90sccm of H_2 for 3 minutes. After that time the H_2 flow is decreased to 30 sccm and these conditions are maintained for 5 minutes. This cleaning process helps to remove the silicide formation taking place on the filament and consequently the life time of the filament is increased.

With the used deposition parameters the thickness of each layer is around:

- p-layer: 25 nm;
- i-layer: 275 nm;
- n-layer: 30 nm.

The most used Si structure is the a-Si:H because its high light absorption makes it possible to have a total cell thicknesses below 1μm. However it has the disadvantage associated with light induced degradation of the material (Staebler-Wronski effect), making its electrical properties to degrade with the incident light due the defects generation. This demands a very good quality intrinsic layer with low defects content.

The cells were deposited with a mask over the ZnO:Al. The mask is a strip with dimensions 3,5cm x 1,0cm (figure 2.9).

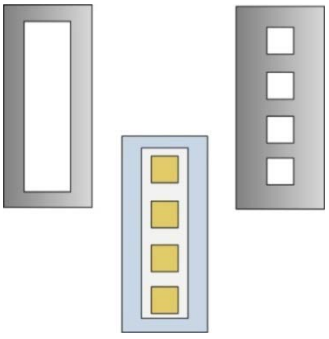

Figure 2.9 Used masks for cells deposition and resulting cells format.

The back reflector and back contact of the cell is composed by a film of aluminum (Al) evapourated over the n-layer and with a very thin protective coating with

nichrome (figure 2.10) (the use of nickel-chromium gave high series resistance to the cells due to its high resistivity, this was a wrong choice for the protective coating. Nickel-vanadium is the best material that can be used). The metallic layers were deposited with a mask of four 0,5cm x 0,5cm squares (figure 2.9).

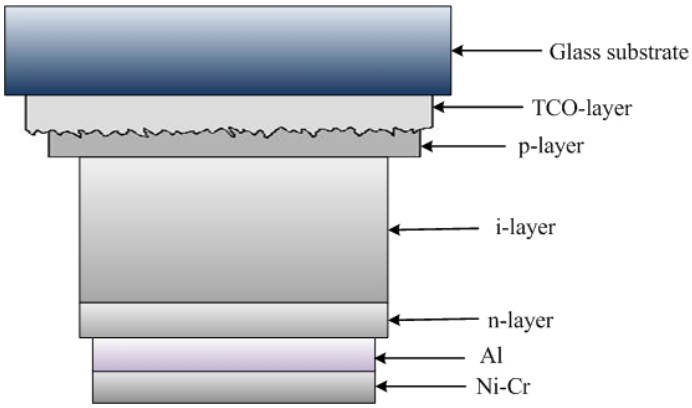

Figure 2.10 a-Si:H cell structure.

With this procedure, four cells were fabricated over textured ZnO:Al films and after their characterization by studying the IV-curve, the quantum efficiency, the fill factor, the open circuit voltage and the short circuit current, the best were chosen to compare their performance with the morphological characteristics.

2.5. Electrical characterization of the thin films

The electrical characterization of the thin films was carried out using the four point probe method. In this technique a current (*I*) is passed through an outer pair of electrodes while the voltage (*V*) between the electrodes of the inner pair is measured (figure 2.11). For a three dimensional conductor, the resistance (*R*) is given by equation 2.1, where ρ is the resistivity of the film, l the spacing between the electrodes, A its cross-sectional area and d the thickness. R_s is the sheet resistance of the film and w the width ($A = d \times w$).

$$R = \rho \times \frac{l}{A} = \frac{\rho}{d} \times \frac{\mathrm{l}}{\mathrm{w}} = \rho = R_s \times \frac{1}{w} \qquad (2.1)$$

Resistivity is a particularly important semiconductor parameter because it can be related directly to the impurity content of a sample, and the four point probe is the apparatus typically used to determine bulk resistivity. With the four probe technique it is possible to measure directly the sheet resistance (R_s) of the thin film. For a very thin layer (thickness d << s) and in the case of a semi-infinite thin sheet, it is given by equation 2.2.

$$R_s = \frac{\pi}{\ln(2)} \frac{V}{I} \tag{2.2}$$

The sheet resistance was measured with a Jandel RM3 test meter, in ohms per square, Ω/□. R_s may be interpreted as the resistance of a square sample, and for this reason the units of R_s are taken to be ohms-per-square or ohm/□. Dimensionally this is the same as ohms but this notation serves as a convenient reminder of the geometrical significance of sheet resistance.

The film's resistivity (ρ) can be calculated from R_s using equation 2.2:

$$\rho = R_s \times d \tag{2.2}$$

where d is the film thickness and ρ units are Ωcm.

So, it is expected that R_s increases with increasing etching time due the decreasing thickness, since ρ is a property of the material. It is considered that the sheet resistance for a TCO of high quality should not be greater than 10 Ω/□.

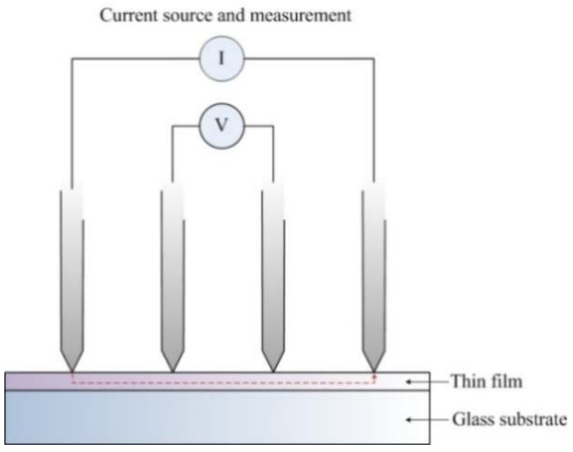

Figure 2.11 Four point probe method for measuring the sheet resistance of a thin film.

The influence on the properties of the etched films due its orientation during the etching was studied. The sheet resistance was measured in three points – both ends and center of the film – as an indication of the film thickness along the glass. The values of these three points, before and after the etching, are shown in Chapter 3, where point 1 is the upper end of the sample, point 2 is the center and point 3 the bottom, in the case of vertical orientation (figure 2.12).

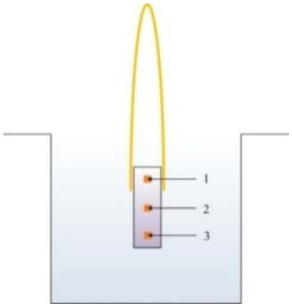

Figure 2.12 Vertical etching with the measurement points.

2.6. Optical characterization of thin films

The optical characterization of the films was performed by measuring the total transmittance, diffuse transmittance and the calculation of the haze parameter, to evaluate the variation of these variables with the etching time and hence with the texture characteristics. The measurements were done in Facultat de Química de la Universitat de Barcelona, with a uv-vis-nir spectrophotometer with an integrating sphere (Perkin Elmer Lambda 19). An integrating sphere is an optical component composed by a spherical cavity which is covered with a scattering material with high reflectivity (i.e., white), except the small holes needed for the entrance of light, to place the sample and the detector. To measure the diffuse light it is necessary to open a port, so the light that is not scattered escapes (figure 2.13).

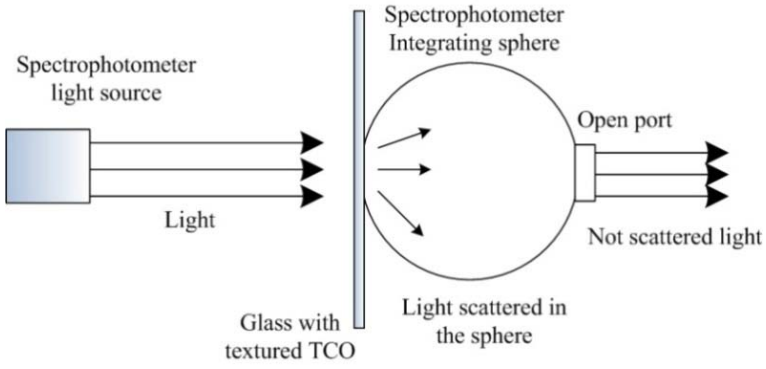

Figure 2.13 Diffuse light measurement in integrating sphere.

As said before, the haze parameter is the ratio between diffuse and total transmittance, so the haze graphs were plotted.

2.7. Morphology analysis (AFM and SEM)

The morphological characterization of the textured ZnO:Al thin films was performed with an **A**tomic **F**orce **M**icroscope (AFM) and a **S**canning **E**lectron **M**icroscope (SEM).

The used atomic force microscope was a Pacific Instruments system and the software for data analyses was XEI 1.7.3 of Psia Inc.

In AFM technique a micro scale cantilever with a sharp probe in its end is used to scan the sample surface. The interaction forces between the probe and the sample surface induce the deflection of the cantilever. These deflections are precisely measured via a laser spot reflected on the cantilever´ top and thus the value of the forces are obtained. These forces depend on the distance between the probe and the surface and hence it is possible to obtain topographical maps of the surface.

One of the parameters that can be obtained with AFM is the rms of the surface roughness, with which the vertical elevation is measured, and is defined as (equation 2.3):

$$\sigma_{rms} = \sqrt{\frac{1}{N}\sum_{i=1}^{N}\left(z_r(x_i)\right)^2} \tag{2.3}$$

where N is the total number of the image and z_r is the relative elevation of each x_i point, relating to the mean value of the height of all points, z (equation 2.4).

$$z_r(x_i) = Z(x_i) - \bar{z} \tag{2.4}$$

SEM is an electron microscope that constructs the image of the sample by scanning it with an electron beam of high energy, which interacts with the sample's atoms. The used SEM is a Hitachi S-4100 (Field Emission) .

In this work, a MATLAB program was also developed to estimate the periodicity of the pyramids of the texturized surfaces, in other words, to calculate the average distance between all the peaks detected in the AFM images.

2.8. Solar cell characterization

The current-voltage characteristics and the quantum efficiency of the solar cell were measured using the set up developed at the Solar Energy group at University of Barcelona. The solar cell was characterized using Newport solar simulator with AM 1.5 filters.

3. Results

This chapter presents the main experimental results of the wet-chemical etching of the ZnO:Al thin films with dilute HCl and their electrical, optical and morphological properties. The results of the application of these films in a-Si:H solar cells are also described.

3.1. Properties of ZnO:Al

3.1.1. Electrical properties

The as-deposited ZnO:Al samples were etched with different times of attack. Even with naked eye it was possible to see the differences between an etched and a flat (non-etched) film. The flat film had a transparent appearance, while the etched ones had a milky appearance. The milky appearance of the etched films became more pronounced with increase in etching time. This is an indication that the roughness of the films increases and more diffusion of the light occurs.

Table 3.1 Sheet resistances at three points for vertically etched films.

Vertical etching		**Sheet Resistance (Ω/□)**	
Etching time (sec)	**Point**	**Before**	**After**
10	1	9,7	16,2
	2	11,6	21,2
	3	15,8	38,9
15	1	7,9	14,0
	2	8,8	17,1
	3	11,1	23,5
20	1	8,3	18,4
	2	9,3	21,2
	3	10,6	45,7

Etchings with the sample held vertically to the acid surface and with the sample held horizontally to it were performed to understand if there are significant differences in the etching behavior in these two cases. In table 3.1 are presented the values of the sheet resistance for the vertical mod of etching.

As expected, the R_s of all films increased with the etching time. However, it was observed that after the attack, in the case of vertical etching, R_s was not uniform. It was relatively high at the bottom end, meaning that this part of the film was more etched and hence had a much thinner film resulting in a higher sheet resistance.

For the horizontal etching the R_s values for the 3 points (both ends and center of the sample) are shown in table 3.2.

Table 3.2 Sheet resistances at three points for horizontal etched films.

Vertical etching		**Sheet Resistance (Ω/□)**	
Etching time (sec)	**Point**	**Before**	**After**
10	1	9,7	16,2
	2	11,6	21,2
	3	15,8	38,9
15	1	7,9	14,0
	2	8,8	17,1
	3	11,1	23,5
20	1	8,3	18,4
	2	9,3	21,2
	3	10,6	45,7

In the case of horizontal etching, the sheet resistance valued did not vary much compared to the values for the vertical etching, meaning that the horizontally etching gave more uniform properties, since the whole surface was immersed and released from the solution approximately at the same time. For a better visualization of this the sheet resistances of the three points in both the cases are shown in figure 3.1 and figure 3.2.

For both horizontal and vertical cases, the R_s values for the 3 points before the etching are different. It happens because the films' homogeneity achieved with the r.f.

deposition is not perfect. However, for the present variation range, the values are considered homogeneous.

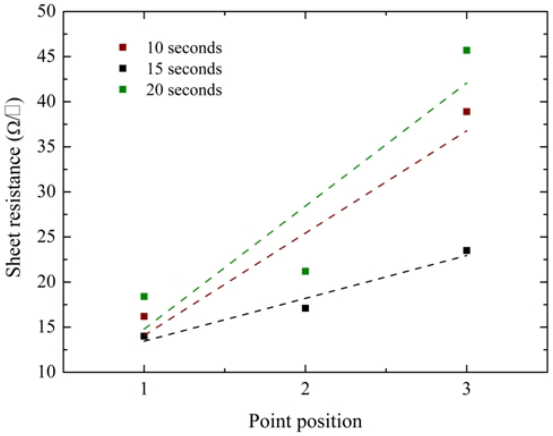

Figure 3.1 Sheet resistances at different points after vertical etching.

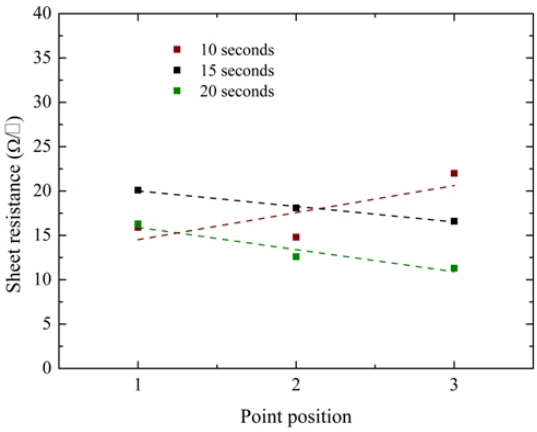

Figure 3.2 Sheet resistances at different points after horizontal etching.

The films that had best electrical homogeneity were chosen to be applied in solar cells. These were the horizontally etched ones and the average R_s values of the three points before and after the etching are shown below in table 3.3 for comparison.

There were ZnO:Al thin films deposited with two different recipes. The difference between the two depositions was mainly in the sputtering power. The first series of the films were deposited with an r.f. power of 150W, while the second series was deposited at 200W. The as-deposited flat ZnO:Al thin films of these two series were called F1 and F2, respectively. These films were used for the chemical etching and the details of the etching are given in table 3.3 with their corresponding sheet resistance before and after etching.

Table 3.3 Average sheet resistance of the films applied in solar cells.

		Sheet Resistance (Ω/□)	
Sample	**Etching time (sec)**	**Before**	**After**
H10	10	10,4	16,0
H15	15	9,2	18,4
H20	20	6,7	13,0
V20	20	9,4	29,4

The H20 sample (20 seconds horizontal etching) was made from the as-deposited films of the F2 series. H10 (10 seconds horizontal etching), H15 (15 seconds horizontal etching) and V20 (20 seconds vertical etching) were made from the as-deposited films of the F1 series.

The relative change in sheet resistance after the etching of the H20 sample is lower than that of H10 or H15. The sheet resistance increase by double the initial value in the case of H15, where the etching time was 15 sec. In the case of H20 made from the ZnO:Al films of the F2 series, 20 sec etching time was needed to change the sheet resistance from 6,7 to 13 Ω/□. This is mainly due to the difference in film quality which reflects in the etching behavior.

The sheet resistances of all the etched films were measured 48 hours after the etching at the same points, and no significant differences were observed compared to the initial values. This reveals the films were stable after the etching process and the rinse method was effective and no acid traces were left on the surface, and hence the sheet resistance did not vary.

3.1.2. Optical properties

To study the influence of the etching time on the optical properties of the ZnO:Al thin films, the total and diffuse transmittance were measured and the haze parameter was calculated.

3.1.2.1. Total transmittance

As mentioned before, the properties of the as-deposited films in the F1 series were different than that of the films in the F2 series. The curves in figure 3.3 show the transmittance spectra as a function of wavelength from 250 to 2500 nm for the as-deposited ZnO:Al flat films made with series F1 and F2.

The F1 series presents a higher transmittance compared to F2. The deposition power was different in these two cases and this resulted in different film properties. The films deposited with F2 conditions showed a higher free carrier absorption compared to F1 in the near infra red (n-IR) region. This was due to the higher deposition power used

for the F2 samples. This also explains why the F2 series films showed lower sheet resistance compared to F1 series films.

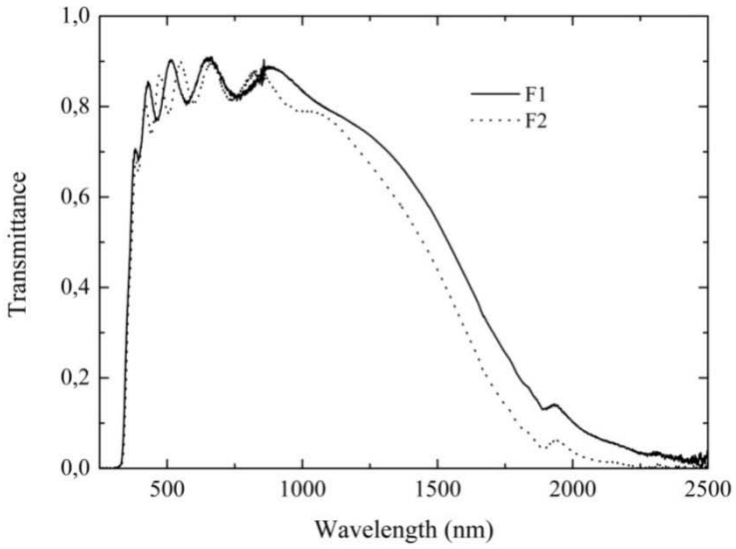

Figure 3.3 Transmittance spectrum of the two ZnO:Al flat film series.

The total transmittances of the ZnO:Al substrates applied in solar cells are presented in the figure 3.4, where H20 does not appears since no measurements were done for this sample. Here, as a matter of identification and comparison, F1 is given as the as-deposited flat ZnO:Al film deposited with the series F1.

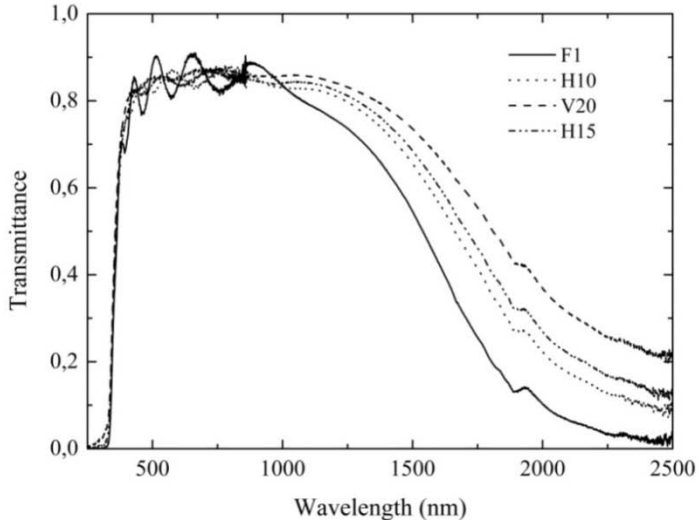

Figure 3.4 Total transmittance of the as-deposited flat and etched ZnO:Al thin films.

The transparency of the ZnO:Al films increased with etching in the n-IR region of wavelength. This might be due to the thickness reduction in the film, which in turn

decreases the doping materials in the bulk resulting in a lower free carrier absorption in the n-IR region.

The average transmittance of the films in the visible range of light (380 to 750 nm) is shown in table 3.4. All the samples showed transmittance higher than 83% in the visible range of light.

Table 3.4 Average % - Transmission of the films in the visible range of light.

Samples	Etching time (seconds)	% - Transmission
F1	-	83,71
H10	10 horizontal	83,04
H15	15 horizontal	83,54
V20	20 vertical	84,57

3.1.2.2. Diffused transmittance

Figure 3.5 shows the diffused transmittance spectra as a function of wavelength for the ZnO:Al samples.

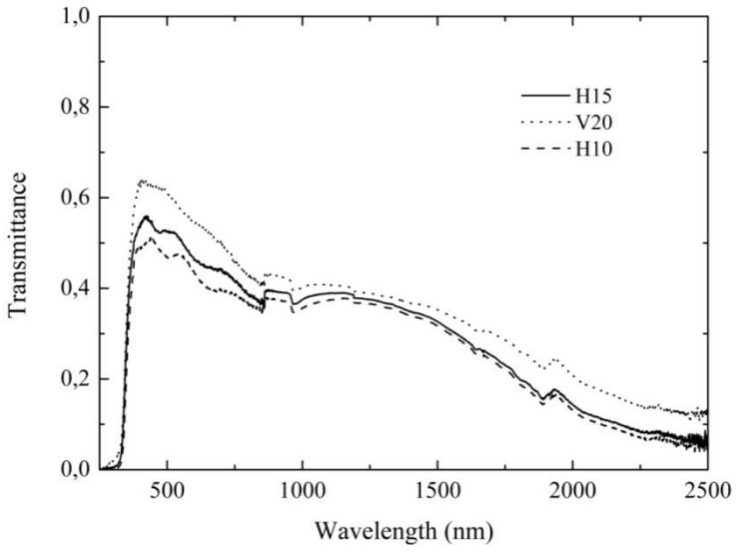

Figure 3.5 Diffuse transmittances of the etched ZnO:Al thin films.

The diffused transmitted light by the samples increases with increase in etching time. The samples become rougher with the etching and the light will be more scattered by this rough surfaces resulting an increase in diffused transmittance.

3.1.2.3. Haze parameter

The haze parameter is the ratio obtained by dividing the diffused transmittance with total transmittance of the TCO. This gives the fraction of the incident light that is scattered incoherently. Figure 3.6 shows the haze values of the as-deposited flat and textured ZnO:Al thin film. In the case of the a-Si:H solar cells the absorption becomes very small above 1000 nm (figure 1.13), and hence the range of important wavelengths is considered only up to 1000 nm. In the visible range of wavelength of light, the haze values were found to depend on the etching time of the ZnO:Al thin films, increasing proportionally with etching time. The film F1 is the one that scatters less light since it is flat.

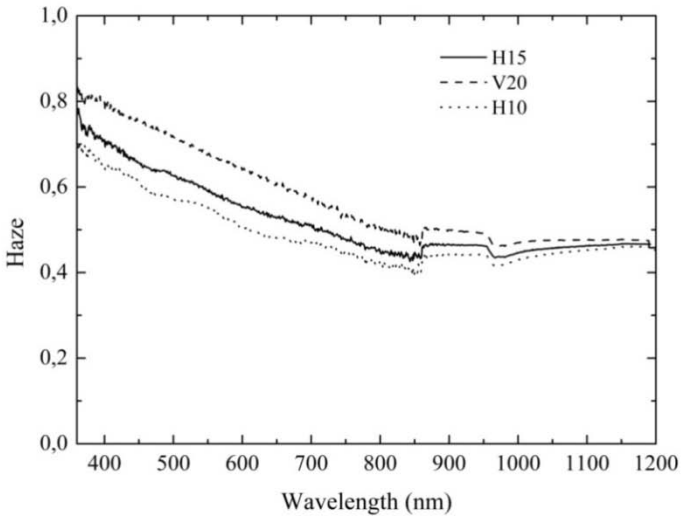

Figure 3.6 Haze values of the as-deposited flat and etched ZnO:Al thin films.

The % Haze value at 600 nm for the etched ZnO:Al films are shown in table 3.5.

Table 3.5 Haze values at 600nm of the etched ZnO:Al thin films.

Samples	Etching time (seconds)	% - Haze
H10	10 horizontal	50,76
H15	15 horizontal	55,51
V20	20 vertical	64,27

3.2. Application of textured ZnO:Al in a-Si:H thin films solar cells

The results of the amorphous silicon thin film solar cells fabricated over the textured ZnO:Al thin films are presented in this section. The objective was to understand the influence of the morphology of the ZnO:Al substrates in the performance of the cells. The substrates used to deposit the cells were H10, H15, H20, V20, F1 and the commercially available Asahi-U (SnO_2:F) substrates.

A photograph of the a-Si:H solar cells deposited over flat and etched ZnO:Al substrates are showing in figure 3.7 (A). The three steps of the fabrication of the cell are visible in the image: the TCO film is deposited all over the glass; the cell (p, i and n-layers) are visible in the strip on the centre of the glass; the four contacts, completing the four cells, are the golden squares. In figure 3.7 (A), the left image (c) represents the cells deposited over a flat ZnO:Al thin film and the right image (d) is that of the cells deposited over etched ZnO:Al film. A scheme of the cells' layers is present in figure 3.7 (B).

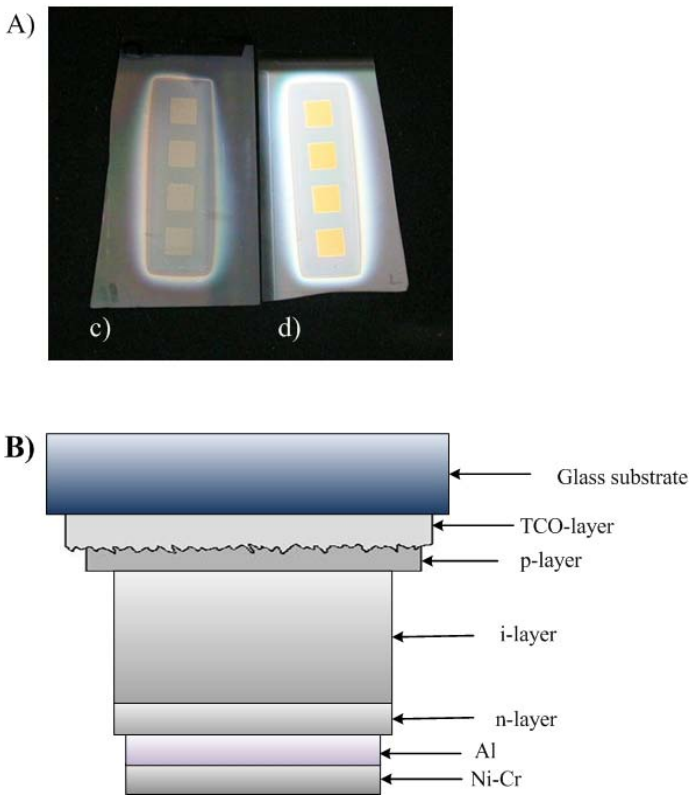

Figure 3.7 Photograph of solar cells (A) deposited over flat (c) and textured (d) ZnO:Al. (B) represents the cell configuration.

3.2.1. Electrical characteristics of the solar cell

The performances of the solar cells were compared by measuring the current-voltage characteristics and also by measuring the external quantum efficiency. Figure 3.8 shows the measured external quantum efficiencies (EQE) of the cells deposited over the flat and textured ZnO:Al substrates as mentioned in the previous sections.

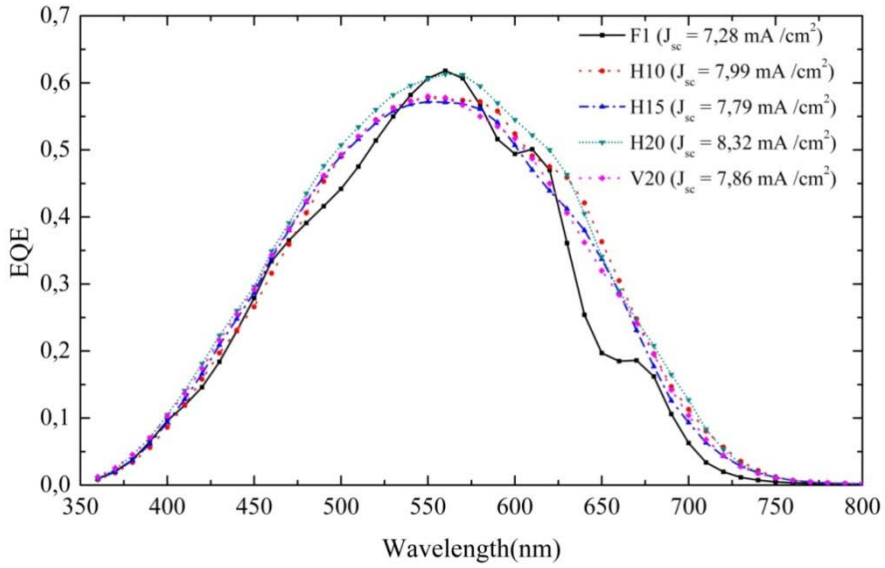

Figure 3.8 EQE of the a-Si:H solar cells fabricated over flat and textured ZnO:Al substrates.

The EQE measurements showed that all the cells deposited over the textured ZnO:Al substrates have higher yield compared to the cells deposited on flat ZnO:Al substrate. The gain was mainly in the longer wavelength region, which suggested an improvement in the light absorption in this wavelength due light trapping. The short circuit current density (Jsc) was estimated from the EQE curves and is given in table 3.6.

Table 3.6 Short circuit current densities of the a-Si:H solar cells deposited over ZnO:Al and Asahi-U substrates. The J_{sc} values of the cells were measure from EQE.

	F1	H10	H15	H20	V20	Asahi-U
Jsc (mA/cm^2)	7,28	7,99	7,79	8,32	7,86	8,07

Analyzing the cells deposited on the 20 seconds vertical and horizontal etched films, it can be seen the horizontal one has a higher EQE than the vertical, which confirmed that horizontal etching is better than the vertical. The higher short circuit current was obtained for the cells deposited on H20 substrate, i.e., the ZnO:Al film etched for 20 sec in the horizontal direction. The cell deposited over this H20 showed higher J_{sc} (8,32 mA/cm^2) than the cells over the commercial Asahi-U substrate (8,07 mA/cm^2). The figure 3.9 compares the EQE of the cells deposited over the Asahi-U and H20 ZnO:Al substrate.

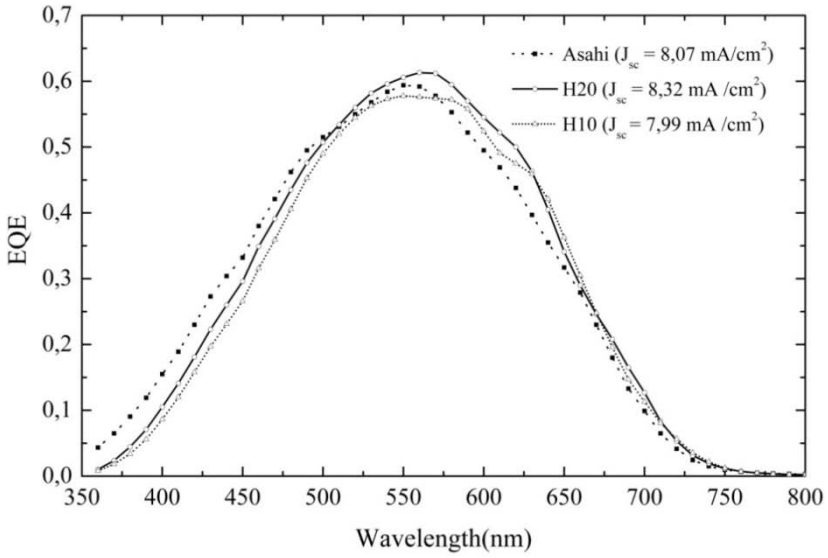

Figure 3.9 EQE of the a-Si:H cells deposited over textured ZnO:Al (H20) and Asahi-U TCO.

Even though the cells on textured ZnO:Al substrates showed higher J_{sc} than the ones on Asahi-U substrate, the cells on Asahi-U showed higher yield in the lower wavelengths as it can be seen in figure 3.9. This might be due to the differences in the TCO-p layer interface of the cell, which needs further optimization in the case of ZnO:Al substrates.

In the silicon thin film solar cells, the texture of the ZnO:Al front surface is transferred to the other cell layers. The textured front surface along with the reflections at the back metal layer contributes to the light capturing efficiency of the device.

The gain obtained with the scattering and reflection in the cells ($J_{sc\ gain}$) was calculated from the J_{sc} of two identically deposited cells: one with a flat front TCO and other with a textured front TCO (equation 4.1) [20].

$$J_{sc\ gain} = \frac{2(J_{sc2}-J_{sc1})}{(J_{sc2}+J_{sc1})} \quad (4.1)$$

In equation (4.1) J_{sc2} is the short circuit current density of the cell deposited on the textured substrate and J_{sc1} is the short circuit current density for the cell deposited on the flat substrate. The calculated values of the $J_{sc\ gain}$ for the cells deposited on different textured ZnO:Al substrates are shown in table 3.7. The H20 textures gave the highest current gain of 13.42%.

Table 3.7 Gain in short circuit current densities of the a-Si:H solar cells deposited over ZnO:Al.

	F1	**H10**	**H15**	**H20**	**V20**
$J_{sc\ gain}$ (%)	-	9,29	6,76	13,42	7,72

The IV curves of the solar cells are presented in figure 3.10. The solar cell characteristics (Jsc, Voc, FF, and efficiency) of the a-Si:H cells fabricated on the flat and textured ZnO:Al substrates along with that on Asahi-U are given in table 3.8. The V_{oc} values were found to be around 0,7 V for the cells deposited over the flat and horizontally etched ZnO:Al substrates. The variation observed in the case of H15 substrate, might be due to some error during the cell fabrication. The cells deposited over the Asahi-U substrates showed less V_{oc} (0,64 V) compared to the cells on ZnO:Al substrates. The best cell obtained were those fabricated over sample H20 of ZnO:Al substrates, with an efficiency of 3,31%. The series resistance of the cells was higher and affected the FF value. The high series resistance was due to the high resistance of the Ni-Cr layer used as the protective metal coating which was a wrong choice. The low thickness of ZnO:Al used in the solar cells might had also contributed to the series resistance. The fill factor value of cells on Asahi-U substrate were higher than that for the cells on the ZnO:Al substrates.

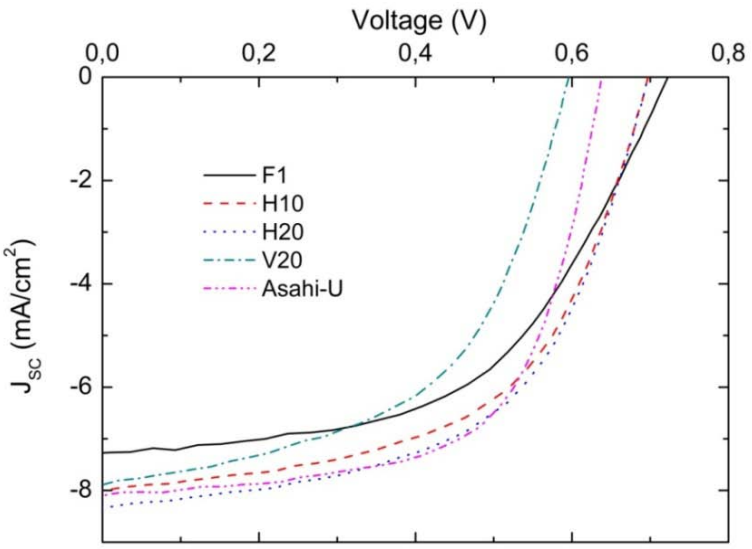

Figure 3.10 I-V curves of the cells deposited over textured ZnO:Al and Asahi-U substrates.

The used Asahi-U substrates had a sheet resistance lower than 10 Ω/□, whereas the lowest sheet resistance for the textured ZnO:Al films used was 13 Ω/□ (H20 sample).

Table 3.8 Characteristics of the a-Si:H solar cells fabricated on different substrates.

Parameters	F1	H10	H15	H20	V20	Asahi-U
J_{SC} (mA/cm^2)	7,28	7,99	7,79	8,32	7,86	8,07
V_{OC} (V)	0,72	0,70	0,57	0,71	0,60	0,64
FF	0,53	0,56	0,29	0,56	0,53	0,63
Efficiency (%)	2,78	3,13	1,29	3,31	2,50	3,25

3.2.2. Morphology analysis

The morphology of the films textured ZnO:Al films were analyzed using scanning electron microscopy. Figure 3.11 shows the SEM images of ZnO:Al thin films before and after the etching (figure 3.11 (A) and (B), respectively). The SEM images showed that the etched ZnO:Al thin films were having randomly distributed craters throughout the surface.

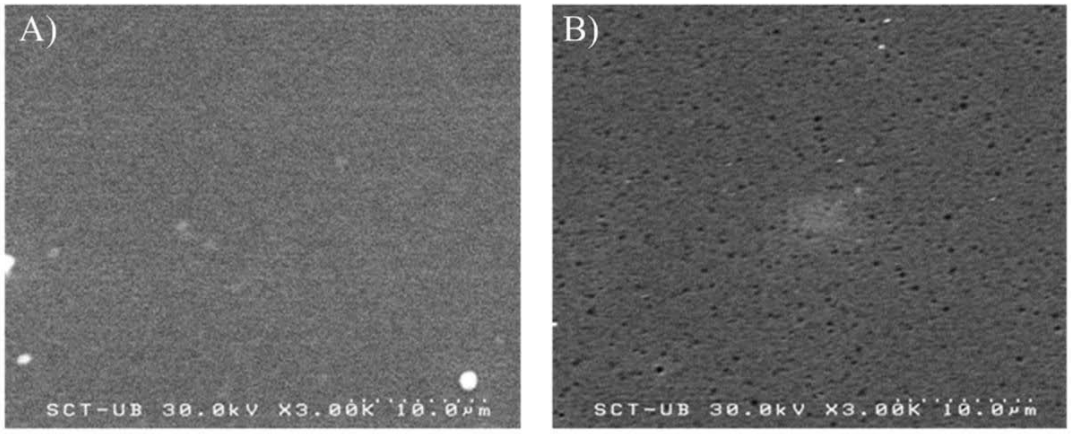

Figure 3.11 SEM images of ZnO:Al thin films before (A), and after etching (B).

The morphology of the solar cells was analyzed using atomic force microscopy (AFM). The AFM measurements were taken over the metallic back contact of the cell and analyzed with the software XEI 1.7.3 of Psia Inc. The morphology observed on the images showed that the texture of the ZnO:Al film was transferred to the consequently deposited layers. The AFM images of all the solar cells deposited as mentioned in last section are presented in figure 3.12 and figure 3.13.

The AFM images showed reflector metal surface has a nano texture that was transferred through the layers by the textured ZnO:Al TCO. The texture of the back metal reflector follows the texture of the front ZnO:Al. The textures have an inverted pyramidal shape which is the characteristics of the etched ZnO:Al. The scan length of all samples was 10 μm x 10 μm.

Figure 3.12 shows the evolution of the surface morphology with the etching time. The HCl etching resulted in a regular roughness morphology lunar landscape like, with some large etch craters that are spread randomly, also present in the ZnO:Al films (figure 3.11). These were present in all the cells deposited over ZnO:Al etched films and not in the Asahi film (SnO_2:F). Asahi-U had a native texture due to growth process, and consequently the Asahi based cell had a morphology with sharper pyramids than the textures on ZnO:Al. The random craters in ZnO:Al cells indicate there are zones with different growth type in the ZnO:Al films. For application in solar cells these craters must be avoided, providing that the etching does not reach the glass substrate removing completely the ZnO:Al. These large craters significantly influence the effective RMS values.

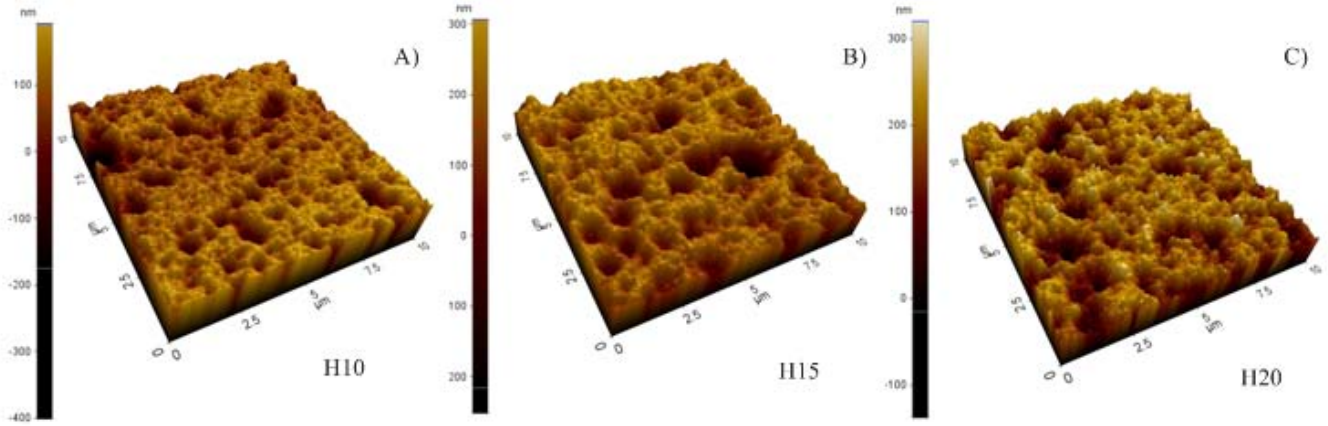

Figure 3.12 AFM images showing the evolution of the textures with etching, of the a-Si:H thin film solar cells. From left (A) cell on H10 (B) cell on H15 (C) the cell on H20

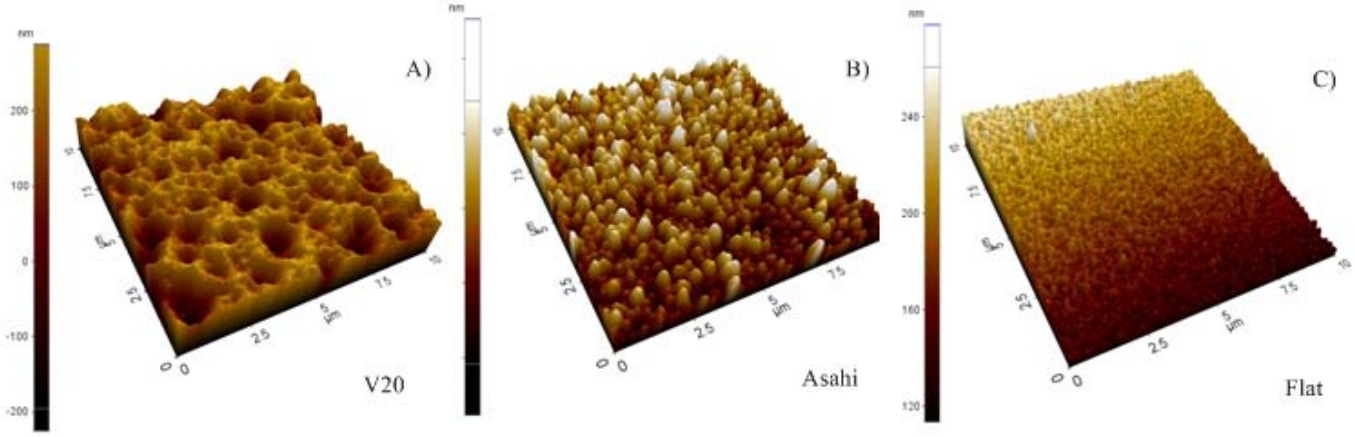

Figure 3.13 AFM images of the surface texture of a-SiH solar cells on different substrates (A) cells on V20,(B) cells on Asahi-U (C) Cells on F1 (flat ZnO:Al).

An example of the depth measure of the holes is present in figure 3.14. The bigger craters showed depths around 260 nm – 380 nm and their number did not change with the etching time. The observed decrease in depth of the larger craters with the etching time must be due to the decrease in the layer thickness. Also, the characteristic opening angle of the large craters is around $\alpha = 21^{o}$.

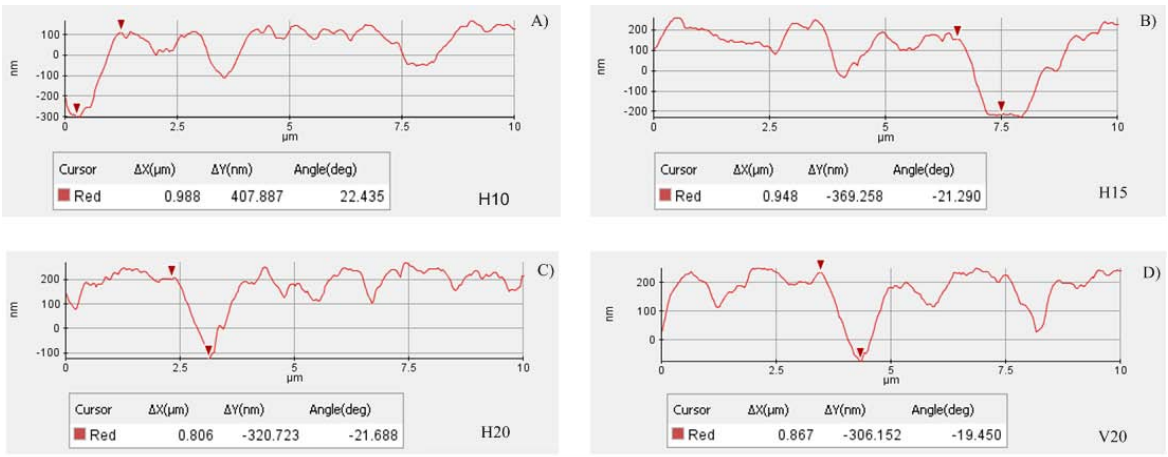

Figure 3.14 Line profile of the depth measurement of the craters in the textures over solar cell surface. (A) cells on H10 (B) cells on H15 (C) cells on H20 and (D) cells on 20V.

The surfaces may be considered irregularly textured, since they can be divided in a sub-texture plus the etch craters. This is illustrated in figure 3.15.

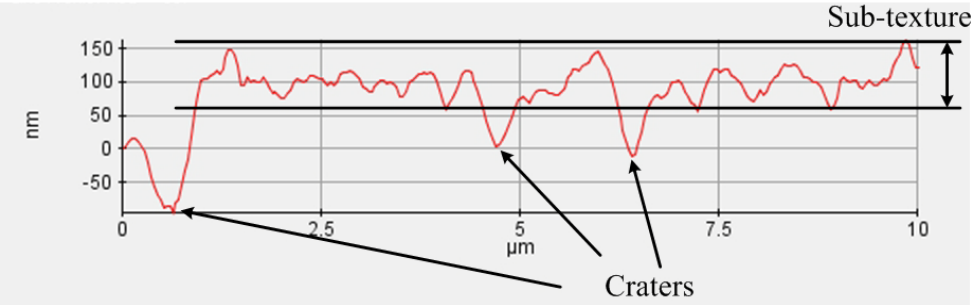

Figure 3.15 Irregularly textured surface of solar cell on H10-ZnO:Al substrate. The surface is characterized by deep craters spread randomly over the surface and a sub-texture.

The RMS roughness values of the different surfaces are shown in table 3.9 for comparison. The values of the best achieved cells are highlighted with a gray background.

Table 3.9 RMS roughness values of the deposited cells.

	F1	H10	H15	H20	V20	Asahi
RMS roughness (nm)	8,06	55, 80	79,78	54,02	79,40	34,17

The flat film had an RMS roughness of 8,06 nm and after the etching treatment, the roughness increased. The RMS roughness of the samples increased when the etching time was increased from 10 to 15 sec, but 20 seconds horizontal etching showed almost the same value like that of 10 seconds. The value for V20 was similar to that on H15. The RMS roughness of the deposited cell over Asahi substrate was 34,17 nm. Although the best value is considered to be around 40 nm, the cells with approximately 55 nm RMS roughness (H10 and H20) showed a good performance compared with the Asahi one. The cells with ~80 nm present a lower J_{sc} and V_{oc}.

3.2.3. AFM image treatment with MATLAB program

A program to measure the average period ($\bar{P}$) (peak to peak distance) of the etched surfaces was developed in MATLAB. With this program it was possible to understand if there was any correlation existing between the periodicity with RMS values, the short circuit current gain (J_{sc}), or with the haze values of different textures. The flow chart of the designed program is present in figure 3.16.

The program uses the AFM images and they are converted into gray scale images, so that image resolution is lower and MATLAB will be faster in processing them. It is necessary to 'find' the maximum intensities, i.e., to determine the intensities corresponding to the peaks in the texture. To determine the maxima: as first step a minimum intensity (I) is chosen and an image is constructed where the intensities below I are set as zero. Then an extended-maxima transform is used, which is defined as the regional maxima of the H-maxima transform, where H is a nonnegative scalar. The regional maxima are connected components of pixels with a constant intensity value, whose external boundary pixels all have a lower value.

Thus, using this transform, a binary image composed by areas with the same intensity, disconnected from each other, is obtained. After choosing I and H, it is necessary to look to the obtained image and decide if it is coherent with the original one, i.e., if it represents the maxima of the original image or not. Then, the centroids of each area are determined, plotted over the binary image and the distances between all points are calculated.

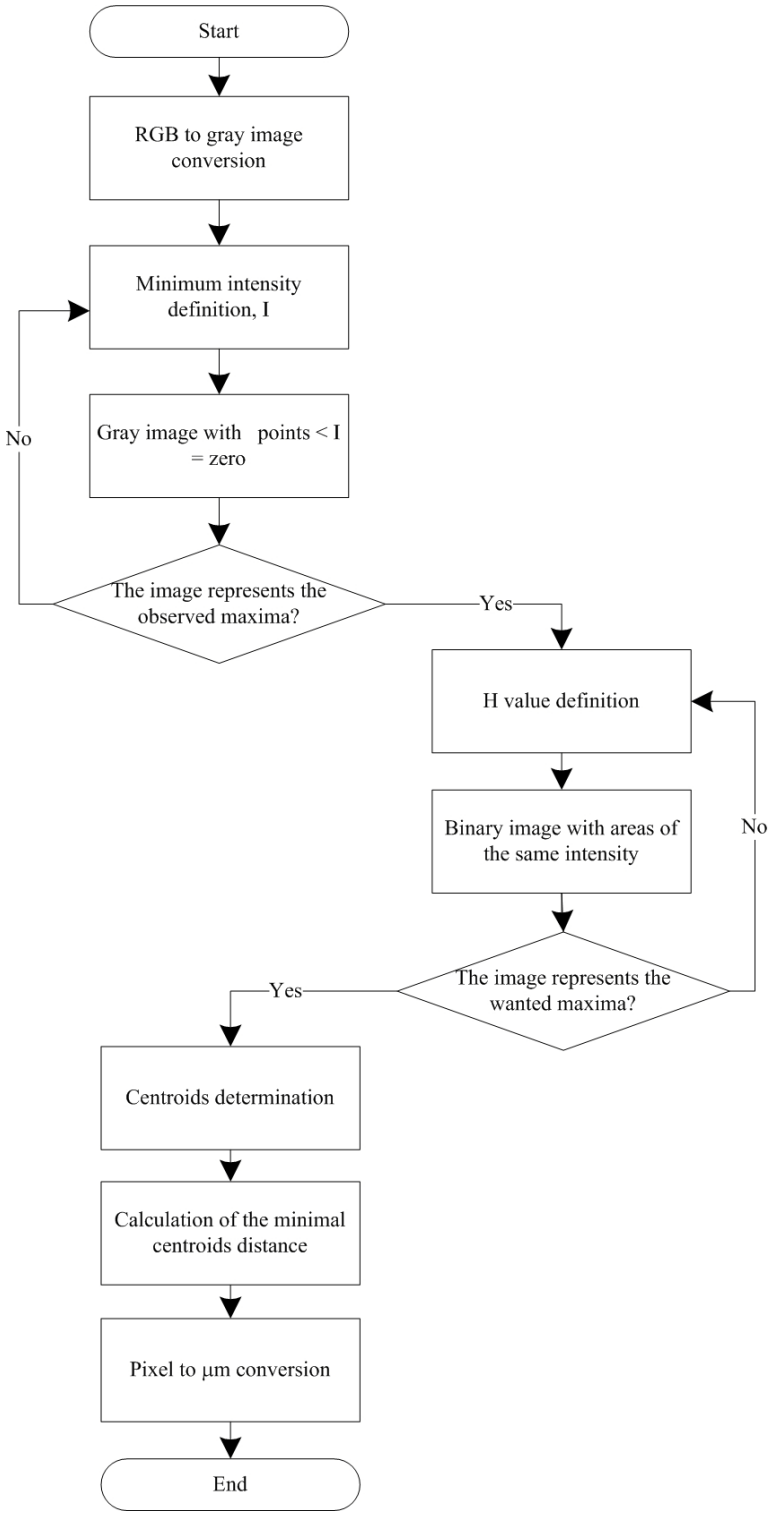

Figure 3.16 Flow chart of the developed MATLAB program for the calculation of average period.

Finally the minimal distance for each point is determined and an average of the minimal distances for all points is made and the conversion from pixels to μm was performed.

Figure 3.17 represents the image evolution of a regular pattern, performed by the program, until an appropriate image to compute $\bar{P}$ is achieved. Observing the images, their evolution leads to image D, which represents the maxima of the original image A. Using the centroids of the areas of image D, the average period is calculated.

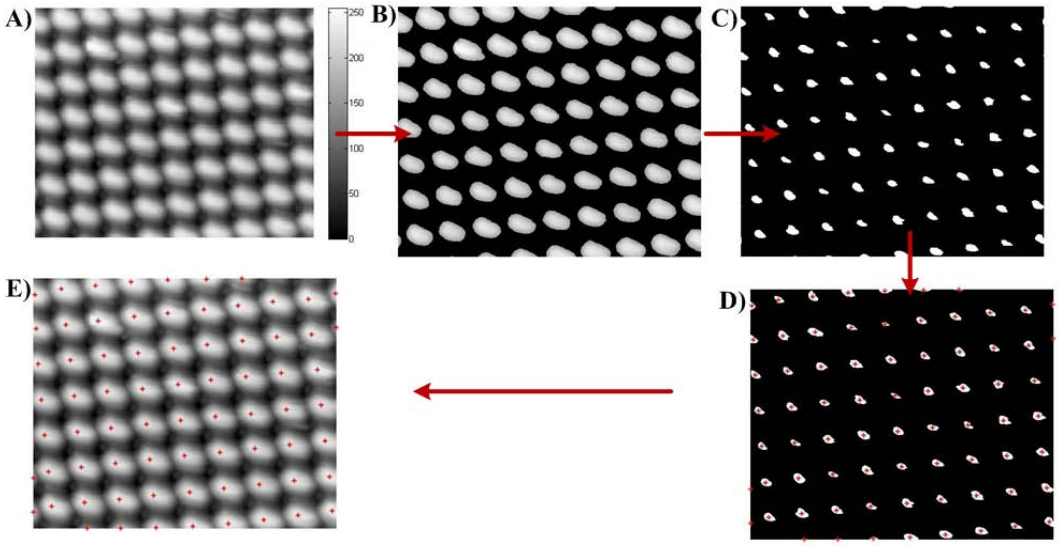

Figure 3.17 Image evolution for calculation of average period.. A) the original image and D) final image with the corresponding centroids.

The obtained value was 1,11 μm which is in agreement with the $\bar{P}$ value measured directly in the image.

Since the achieved ZnO:Al surfaces were very irregularly textured and the etch craters influence the periodicity values, it was hard to define an intensity that covers all the maxima. Therefore it was very difficult to accurately determine the average period. In addition, the quality of the AFM images also influences the measurement. If the image is too blurred and has a poor contrast, it is very difficult to separate the maxima, and the results will not be accurate. To optimize the measurements, the behavior of the program for different H values was analyzed and through a profile measurement with the XEI 1.7.3 program the values obtained were confirmed. In figure 3.18 is shown the line profile of the cell deposited over Asahi-U substrate.

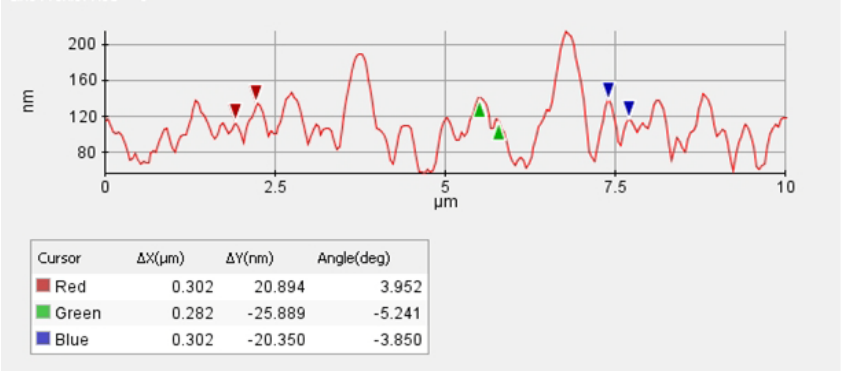

Figure 3.18 Line profile of the textured cell surface deposited over Asahi-U substrates.

In figure 3.18, the Δx parameter is the horizontal distance between cursors of the same color. From the Δx values it was possible to have an idea of the period of the surface, which was around 0,29 µm.

Figure 3.19 shows the images obtained with the MATLAB program to calculate the average period, for I=70 and H=5, for the same solar cell on Asahi-U, discussed in figure 3.18. The obtained average period with the MATLAB program for this cell was 0,28 µm, which is very close to the value estimated by the line profile analysis.

Despite the influence of the large etch craters, an estimate of the $\bar{P}$ values of all the deposited cells were obtained. These values are present in table 3.10. It was found that the average period increases with increase in etching time.

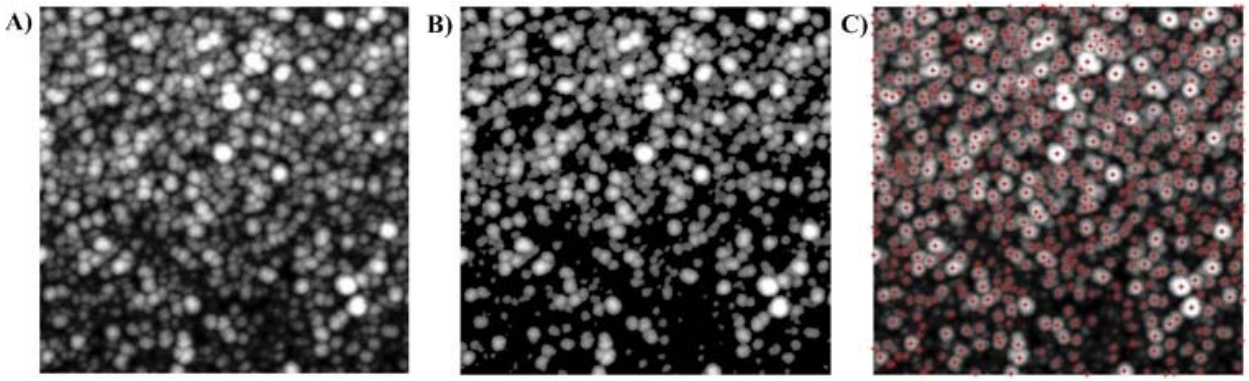

Figure 3.19 MATLAB treatment of the image of solar cell deposited over Asahi-U substrate. Image C represents the centroids of the maxima.

Here, also the cells on H20 shows exception with an average period of 0,26µm which is comparable to that for the cells on Asahi-U substrates. The variation in the

properties of the H20 might be due to the difference in the deposition condition as mentioned earlier in this chapter.

Table 3.10 Average period estimated for the solar cell surface textures on different substrates and its RMS roughness values.

	F1	H10	H15	H20	V20	Asahi-U
J_{sc} (mA/cm^2)	7,28	7,99	7,79	8,32	7,86	8,07
Average period (μm)	0,22	0,35	0,37	0,26	0,42	0,28
RMS roughness (nm)	8,06	55, 80	79,78	54,02	79,40	34,17

Figure 3.20 shows a plot of RMS roughness and haze parameter values against the average period, in order to understand the behavior of this parameters with $\bar{P}$.

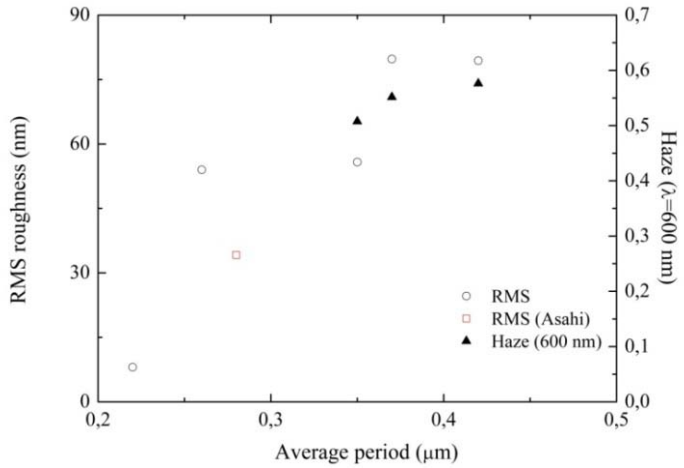

Figure 3.20 Variation of RMS roughness and haze parameter with average period.

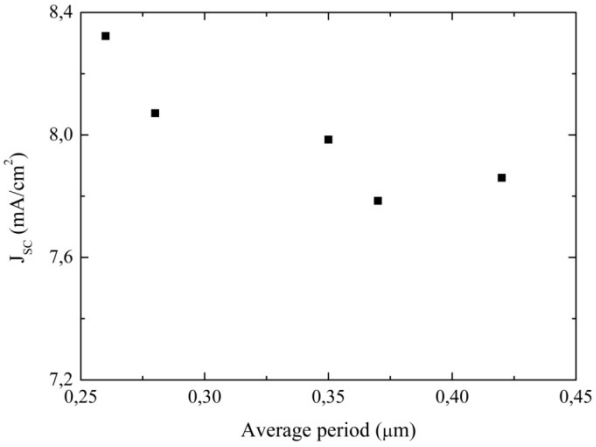

Figure 3.21 Variation of short circuit current (J_{sc}) with average period.

According to the graph, the RMS roughness and the haze parameter increase with increasing average period.

In order to study the effect of average period in the cells, the short circuit current density was plotted against the average period as shown in figure 3.21.

The short circuit current density of the cells was found to decrease with the increase in period. The cells with the lowest average period of 0.26 μm showed the highest J_{sc} value. The results showed that the average period distance is an important parameter which controls the short circuit current density of a-Si:H thin film solar cells.

4. Conclusions and Remarks

The main goal of this thesis was to obtain textured ZnO:Al films with an appropriate texture to be used as a substrate for the deposition of thin films silicon solar cells. The texturing of the ZnO:Al thin films was performed by an easy and economic method; the wet chemical etching with HCl acid (0,5% concentration).

The chapter presents the conclusion of the etching of ZnO:Al thin films and their application in a-Si:H thin film solar cells.

Considering the horizontal and vertical etching of the sample, and analyzing the properties of the resulted films, the following conclusions were made:

- With the etching, the sheet resistance (R_s) of all the ZnO:Al thin films increased, due the decrease in thickness;

- The sputtering conditions have a strong influence in the film etching and the ZnO:Al films (H20) deposited at 200W showed better results than those deposited at 150W;

- Etching was performed by keeping the ZnO:Al films horizontally and vertically, with respect to the acid surface. The sheet resistance values for the vertical etching showed a strong non-homogeneity after etching. The bottom end of the samples showed much higher Rs than the upper end, because the time it was under chemical attack was longer;

- On the other hand, the horizontal etching resulted in homogeneous films with good electrical properties to be used as textured TCOs in solar cells.

The optical characterization of the ZnO:Al thin films were done by measuring the total and diffused transmittance using a spectrophotometer with an integrating sphere. The haze values were calculated from the total and diffused transmittance and the conclusion are presented as follows:

- All the films showed a transmittance above 83% in the visible range of light;

- The total transmittance in the near infra red region was found to increase with the etching time. This behavior might be due to the effective decrease in thickness, which in turns reduced the effective doping level in the bulk of the film, resulted in lower free carrier absorption;

- The diffused transmittance in the visible range of wavelength of light increased with increase in etching time, due to the increase in surface roughness;

- The haze parameter in the visible wavelength of light (i.e., the ratio between the diffused and total transmittance) increased from ~50% to ~64% when the etching time was increased from 10 to 20sec.

After analyzing the ZnO:Al films and their textures, a-Si:H thin film solar cells were deposited over a series of textured films, to study the role of different textures in the cell performance (i.e., external quantum efficiency (EQE), the short circuit current density, (J_{sc}), and IV curve). The conclusions from the cell characterization are given below:

- The cells deposited over the textured ZnO:Al substrates showed higher short circuit current density than that for the flat ZnO:Al substrates;

- The highest gain obtained in the short circuit current density ($J_{sc\ gain}$) by using a textured TCO and a textured back reflector (the roughness of the substrate was transferred to the other layers) was up to 13,42 % with etched ZnO:Al substrate (for a horizontal etching time of 20 seconds). This proved the effectiveness of the etched ZnO:Al films to improve the light trapping in the solar cell;

- The cell deposited over textured ZnO:Al substrate with 20 sec horizontal etching showed better short circuit current and efficiency than commercially available Asahi-U substrate;

- The efficiency of the cells on Asahi-U substrate was 3,25% whereas the cells on textured ZnO:Al showed 3,31%;
- The cells deposited over ZnO:Al substrates showed less light conversion efficiencies in the blue region of wavelength compared to the cells on Asahi-U (SnO_2:F) substrate. This might be due to the difference in the properties of TCO-p layer interface.

The morphological characterization was done using AFM and SEM measurements. AFM measurements were taken over the metallic back contact of the cell after fabrication. Using the developed MATLAB program the average period was estimated. The conclusions of these analyses are:

- The AFM images showed that the texture of the ZnO:Al film was transferred to all layers of the solar cell;

- The SEM and AFM images showed that the etched films have large craters randomly distributed over the surface. This might be probably due to localized growth defects. The obtained surfaces were irregularly textured and can be divided into zones of sub-texture plus large craters;

- The highest values of J_{sc} were obtained for an RMS value around 55,8 nm in the case of textured ZnO:Al films, where as the Asahi-U substrate (SnO_2:F) with around 34 nm RMS roughness showed similar results;

- The average period, $\bar{P}$, was estimated by treating the AFM images with the developed MATLAB program;

- Both the RMS roughness of the surfaces and the haze parameter of the TCOs increase with increasing average period;

- The average period was found to be a critical parameter in the performance of the solar cell. The short circuit current density was found to decrease with increase in average period.

- Higher value for the J_{sc} was obtained for the textured ZnO:Al substrate with average period of 0,26μm followed by Asahi-U substrate with an average period of 0.28μm.

Further studies are necessary to optimize the best texture for the application in silicon thin film solar cells. The deposition conditions of the ZnO:Al was found to be a critical parameter which controls the etching behavior. In the present study the films deposited with an r.f. power of 200W and a substrate temperature of 350 ºC was found to be the best choice. Further studies may be done with films deposited with other process conditions varying power and deposition pressure.

The Angular Distribution Function (ADF) of the light scattered by the textured surfaces will give better understanding of the textured surfaces.

It will be also appropriate to analyze the SEM images (preferably cross sectional SEM) to know the depth to which the craters are formed. These craters spread over the surface may cause a drop in the efficiency of thin film solar cells and hence further studies are needed to eliminate this crater formation. Since the crater formation is due to the in-homogeneities in the as-deposited film, further optimization of the deposition conditions are essential.

5. Bibliography

[1] Green M.A., *Third Generation Photovoltaics: Advanced Solar Energy Conversion*, Springer (2005);

[2] Hirshman W. P., Hering G., Schmela M., *Market Survey: Cell & Module Production*, Photon International (March 2008);

[3] Green M. A., *Solar Cells*, Prentice Hall (1982);

[4] Escarré J., *Tècniques de confinament òptic en cèl·lules solars sobre substrat plàsti*, thesis of Doctoral degree (2008);

[5] Luque A., Hegedus S., *Handbook of Photovoltaic Science and Engineering*, John Wiley & Sons, Ltd. (2003);

[6] Shah A., Schade H., Vanecek M., Meier J., Vallat-Sauvain E., Wyrsch N., Kroll U., Droz C., Bailat J., *Thin-film silicon solar cell technology*, Progress in Photovoltaics: Research and Applications, Vol. 12, pp. 113-142, John Wiley&Sons, Ltd. (2004);

[7] Fortunato E., Ginley D., Hosono H., Paine D. C., *Transparent Conducting Oxides for Photovoltaic*, MRS Bulletin, Vol. 32 (March 2007);

[8] Bashar S., *Study of Indium Tin Oxide (ITO) for Novel Optoelectronic Devices*", thesis of Doctoral degree (October 1997);

[9] Bunshah R., *Handbook of Deposition Technologies for films and coatings*, *2nd edition*, Noyes Publications (1950);

[10] Vilamitjana D., *Amorphous Silicon Solar Cells obtained by Hot-Wire Chemical Vapour Deposition*, thesis of Doctoral degree (September 2004);

[11] Turon M., *Progress in Hot-Wire Deposited Nanocrystalline Silicon Solar Cells*, thesis of Doctoral degree (June 2003);

[12] Poortmans J., Arkhipov V., *Thin Film Solar Cells Fabrication, Characterization and Applications*, John Wiley & Sons, Ltd. (2006);

[13] Birkmire R. W., *Compound polycrystalline solar cells: Recent progress and perspective*, Solar Energy Materials and Solar Cells, Vol. 65, pp. 17-28 (2001);

[14] McLaughlin M., Zisman A., *The Aqueous Cleaning Handbook, 3rd edition*, AL Technical Communications (2002);

[15] Kluth O., Rech B., Houben L., Wieder S., Schöpe G., Beneking C., Wagner H., Löffl A., Schock H.W., *Texture etched ZnO:Al coated glass substrates for silicon based thin film solar cells*, Thin Solid Films, Vol. 351, pp. 247-253 (1999);

[16] Chang S.C., Hicks D.B., Laugal R.C.O., *Patterning of zinc oxide thin films*, Solid-State Sensor Actuator Workshop (New York: IEEE), pp. 41-45 (1992);

[17] Terrazzoni-Daudrix V., Guillet J., Freitas F., Shah A., Ballif C., Winkler P., Ferreloc M., Benagli S., Niquille X., Fischer D., Morf R., *Characterisation of rough reflecting substrates incorporated into thin-film silicon solar cells*, Progress in Photovoltaics: Research and Applications Vol. 14, pp. 485-498 (2006);

[18] Sterling D. J., *Technician's Guide to Fiber Optics, 4th edition*, Delmar Cengage Learning (2003);

[19] pvcdrom.pveducation.org.

Appendix A

Security and hygiene protocol

Since, it was necessary to handle with corrosive, irritant and toxic products, several security procedures were taken into account besides the basic security rules that are followed in a laboratory work.

In the clean room, where the cleaning of the samples and the sputtering deposition were done, it was mandatory to wear special protective clothing (clean room suits) that do not give off lint particles and also avoid human skin and hair particles from entering in the room's atmosphere. They also prevent particles from outside in entering the room, and contaminate the ambient. These materials used to prevent contamination were:

- Latex gloves;
- Mask;
- Booties;
- Clean room suit;
- Head cover.

For the chemical wet etching with HCl, several accessories were used for protection:

- Protection glasses;
- Anti-acid gloves;
- Mask;
- Protection suit.

After the chemical treatments, the used solutions were stored appropriately in their respective containers for their correct posterior treatment.

Appendix B

MATLAB code

```
clear all;
close all;

 1 %Conversion of the rgb image to binary image
 2 Image=input('image:'); %The image name needs to be between ''
 3 D=imread(Image); %Loads the image
 4 A2=rgb2gray(D); %converts the image to gray scale
 5 imshow(A2); %shows the image
 6 I=input('Please enter the minimum intensity you require: ');
 7 [s,l]=size(A2); %gives the size of the A2 image matrix
 8
 9 % constructs the image with the minimum required intensity
10 for o=1:s
11    for p=1:l
12        if A2(o,p)>=I
13            Z(o,p)=A2(o,p);
14        end
15    end
16 end
17
18 figure, imshow (Z);
19
20 %Computes the extended-maxima transform
21 intervalo=input('Please enter H value(regional maxima):');
22 B=imextendedmax(Z,intervalo);
23 figure,imshow(B);
24
25 %Finds the centre of each maxima group
26 C=bwlabel(B); %converts the binary image to a label matrix
27 s=regionprops(C, 'centroid'); %finds the centre
28 centroids=cat(1, s.Centroid); %concatenates
```

```
figure,imshow(C);
hold on
   plot(centroids(:,1),centroids(:,2),'r*')%plots the centers
hold off

%Superimposes the centroids in A2 image
figure,imshow(A2)
hold on
   plot(centroids(:,1), centroids(:,2), 'r*')
hold off

%Calculates the distances between all points
[m,n]=size(centroids);
for k=1:m
  d(k,n)=0;
    for n=1:m
      d(k,n)=sqrt(((centroids(k,1)-centroids(n,1)).^2)+ ...
     (centroids(k,2)-centroids(n,2)).^2));
    end
end

%Calculates the minimal distance for each point
for i=1:m;
    for j=m;
        R=d(i,1:j); %lines of the matrix
        r=unique(R); %values in ascendant order
         min=r(2); %chooses the second smallest value, because
%every line as a 0 value(distance between a point and itself)
    end
     Min(i)=min;
end

%Mean distance and conversion to metric: 512 pixels=10 micro
% -> 1 pixel=0.01953125 micros
Mean_distance_pixels = mean(Min)
Mean_distance_micros=Mean_distance_pixels*0.01953125
```